hearing impairment genes, *GJB3* and *KCNQ4*, have been identified in the DFNA2 locus (Kubisch et al. 1999; Xia et al. 1998). The *KCNQ4* gene consists of 14 exons that encode a protein of 695 amino acids (MIM*603537). The KCNQ4 protein contains six transmembrane domains and a P-loop region that forms the potassium-selective channel pore (Kubisch et al. 1999). Six missense mutations have been reported in the *KCNQ4* gene to date (Akita et al. 2001; Coucke et al. 1999; Kubisch et al. 1999; Talebizadeh et al. 1999; Topsakal et al. 2005; Van Camp et al. 2002; Van Hauwe et al. 2000). Co-expression studies in *Xenopus* oocytes revealed that the mutant channel protein with a missense mutation exerted a strong dominant-negative effect, which may explain the autosomal-dominant inheritance of *KCNQ4* deafness (Kubisch et al. 1999). Besides the missense mutations, one small deletion has also been reported (Coucke et al. 1999). Because the mutation generated a channel protein that is truncated before the first transmembrane domain, it is unlikely that the mutant protein had a dominant-negative effect. The pathogenic mechanism of this deletion in *KCNQ4*, therefore, remains elusive (Coucke et al. 1999). Recently, Topsakal et al. (2005) noted a phenotypic difference among eight pedigrees with six missense mutations and a single pedigree with the c.211_223del mutation. Based on these data, a hypothesis for the genotype–phenotype correlation is suggested in which younger-onset and all-frequency hearing loss is associated with missense mutations, and later-onset and pure high-frequency hearing loss with null mutations. Although it is an attractive hypothesis, more phenotypic information should be accumulated from individuals with other null *KCNQ4* mutations in order to evaluate the genotype–phenotype correlation.

We identified a novel one-base deletion in *KCNQ4* exon 1 in a large Japanese pedigree with hearing loss using genome-wide linkage analysis and candidate gene analysis. Individuals with the deletion manifested later-onset and pure high-frequency hearing loss, compared with reported patients with *KCNQ4* missense mutations. Our observations support the phenotype–genotype correlation in *KCNQ4* deafness, and suggest that haploinsufficiency is the most likely mechanism for development of hearing loss caused by the null *KCNQ4* mutations.

Materials and methods

Family data

A Japanese family affected with autosomal-dominant, nonsyndromic hearing impairment was identified (Fig. 1). All affected family members had an affected and an unaffected parent, and four male-to-male transmissions were noted. Twenty-four members of the family participated in this study after giving informed consent. They were asked to complete a questionnaire to exclude other causes of hearing impairment. Special attention was paid to features that might have caused syndromic hearing impairment. All participants underwent otoscopic and audiological examinations. Pure-tone audiograms were obtained in a sound-treated room. Air conduction thresholds were measured in dB hearing level (HL) at 500, 1,000, 2,000, 4,000, and 8,000 Hz. Diagnosis of progressive sensorineural hearing impairment was based on pure-tone audiogram, questionnaire information, and medical records. Family members were considered to be affected if they had sensorineural hearing impairment of more than 25 dB at more than one frequency. Syndromic hearing impairment and environmental causes of deafness were excluded from this study. The ethics committee of Tohoku University School of Medicine approved this study.

Genetic analysis

Blood samples were obtained from 24 family members, 13 affected and 11 unaffected. Control samples were obtained from 100 Japanese subjects with normal hearing. DNA was extracted from peripheral blood leukocytes using the Genomic DNA purification kit (Promega, Madison, WI, USA). In the genome-wide linkage analysis, microsatellite markers of the Human MAPPAIRS (Invitrogen, Carlsbad, CA, USA) were used for genotyping on the ABI 373A DNA Sequencer. Detailed information for additional genetic markers used in this study can be found in the NCBI Human Map Viewer. We performed pedigree and haplotype constructions using the Cyrillic version 2.1 software. Two-point LOD scores were calculated by the MLINK program of the LINKAGE version 5.1 software package (Lathrop et al. 1984). The affected allele frequency and penetrance were set at 0.0001 and 1.0, respectively. Multipoint linkage analyses were conducted using the GENEHUNTER 2 (Kruglyak et al. 1996).

Mutation analysis was performed by genomic exon sequencing. PCR was carried out using primers flanking 1 *GJB3* exon and 14 *KCNQ4* exons. Reaction conditions were optimized for different primer sets. Primer sequences were based on the genomic sequence available in the Genbank (*GJB3*, AF099730; *KCNQ4*, AH007377). The amplification products from both genes were sequenced with the ABI Prism BigDye Terminator Cycle Sequencing Ready Reaction Kit (Applied Biosystems, Foster City, CA, USA) on the ABI 310 Genetic Analyzer and analyzed using the ABI DNA Sequencing Analysis version 5.1 software.

Results

Genetic analysis

In the genome-wide screening, a maximum two-point LOD score of 5.42 at $\theta = 0$ was obtained for GATA129H04 (penetrance = 1.0, Table 1). In addition, multipoint linkage analysis with GATA129H04 revealed

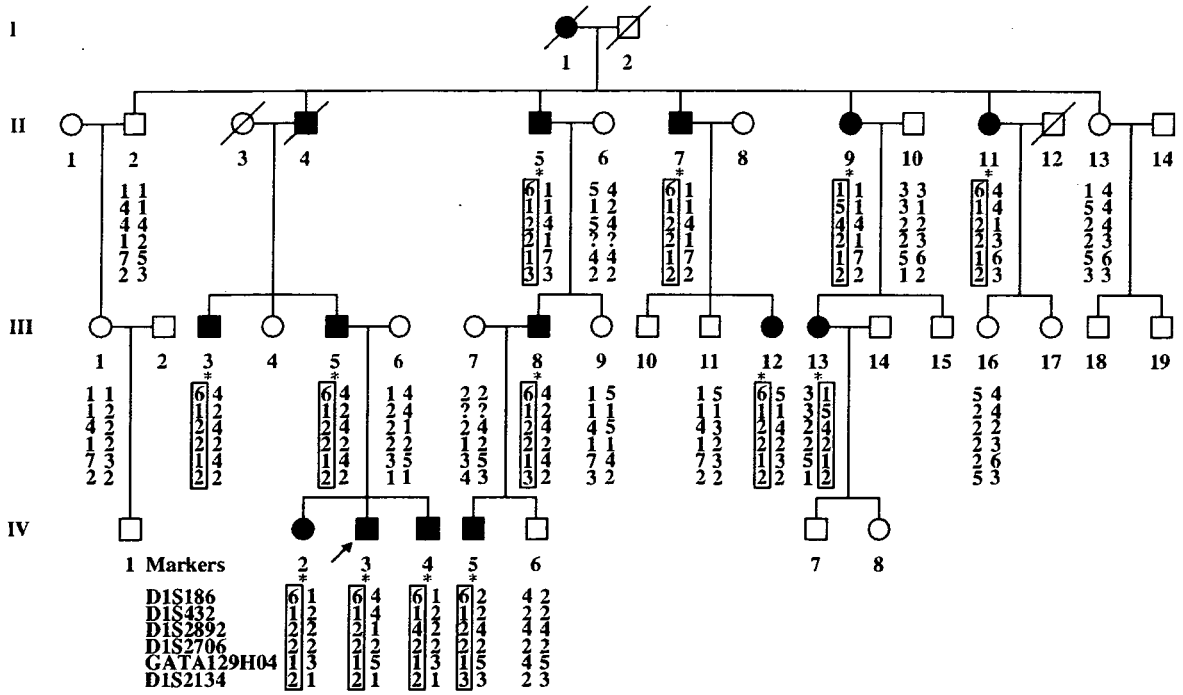

Fig. 1 Pedigree of the Japanese family with nonsyndromic, autosomal-dominant hearing impairment. The *asterisks* indicate those individuals in whom a *KCNQ4* mutation was identified. The haplotype *enclosed in the box* shows the disease haplotype

Table 1 Two-point LOD scores for linkage between hearing impairment and microsatellite markers in a Japanese family

Marker	Marshfield map distance (cM)	LOD score at θ					
		0	0.05	0.1	0.2	0.3	0.4
D1S234	55.10	2.99	2.75	2.49	1.93	1.28	0.59
D1S496	64.38	−999.99	3.09	3.00	2.44	1.64	0.71
D1S186	67.22	−999.99	3.09	2.97	2.35	1.50	0.55
D1S432	69.86	−999.99	0.81	1.13	1.15	0.86	0.44
D1S2892	70.41	−999.99	−1.59	−0.69	−0.10	0.02	0.02
D1S2706	71.13	1.68	1.53	1.38	1.04	0.66	0.25
GATA129H04	72.59	5.42	4.97	4.50	3.48	2.32	1.01
D1S2134	75.66	−999.99	0.73	0.83	0.70	0.45	0.20
D1S200	82.41	−999.99	3.16	3.02	2.36	1.47	0.50

a maximum nonparametric linkage (NPL) score of 10.95 (data not shown). This marker is known to flank the DFNA2 locus on chromosome 1p34. As shown in Fig. 1, the most likely haplotypes were constructed to determine the borders of the critical region. All affected family members shared the same disease haplotype. The recombination between D1S2134 and the gene for hearing impairment was found in family member II-5. In family member II-9, recombination occurred between the gene for hearing impairment and marker D1S2892. These events localized the gene for hearing impairment between D1S2892 and D1S2134. This region is at 1p34, where the DFNA2 locus resides. These data clearly indicated linkage of the hearing impairment to the DFNA2 locus in this family.

As linkage to the DFNA2 locus was proven in this family, both *GJB3* and *KCNQ4* genes were examined for mutations. First, we sequenced the coding region of *GJB3* in this family, but did not find any mutations. Subsequently, we analyzed all *KCNQ4* exons. In exon 1 we identified a deletion of C at nucleotide position 211 of the *KCNQ4* cDNA sequence (Fig. 2). All affected family members were heterozygous for this mutation (Fig. 1). The mutation was not detected in the 100 normal controls.

Clinical features

We performed a clinical study on the Japanese family members (13 affected) with a null *KCNQ4* mutation to delineate its phenotypic features (Table 2). Patients showed a nonsyndromic, postlingual, symmetric and sensorineural hearing impairment. The hearing impair-

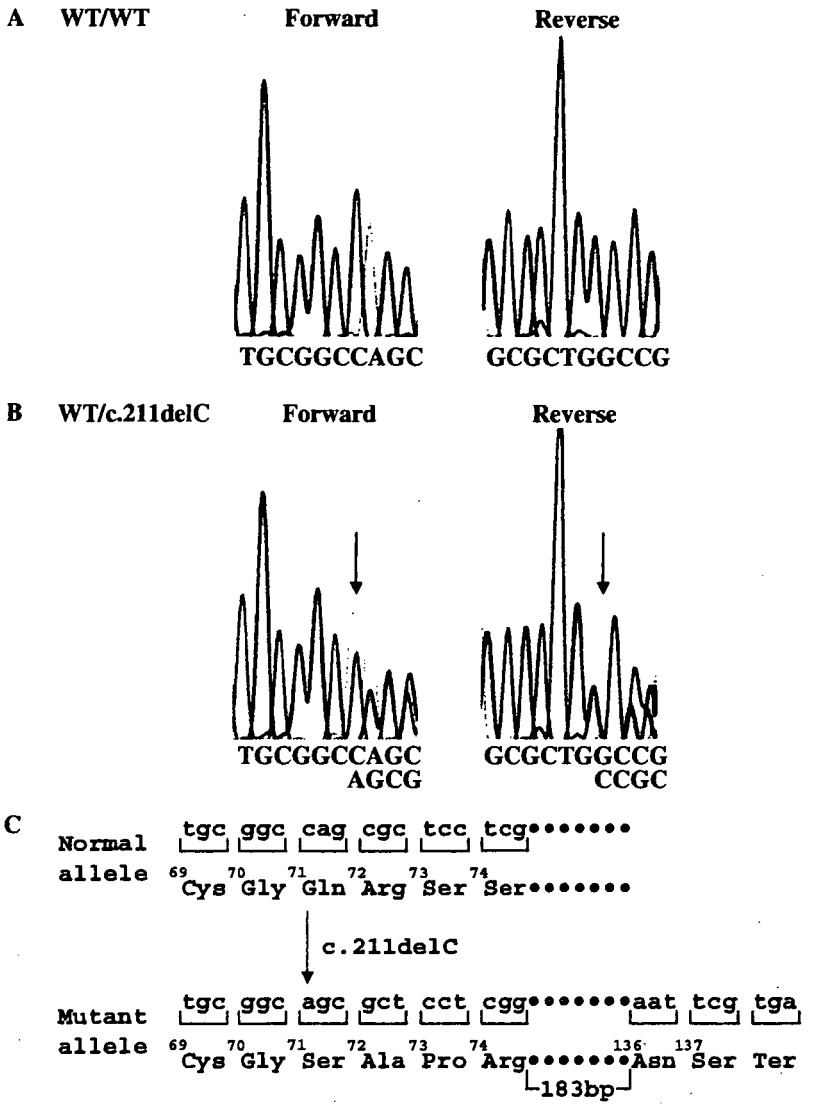

Fig. 2 Sequence analysis of the *KCNQ4* in **a** an unaffected (WT/WT) and **b** an affected member (WT/c.211delC) of the pedigree. The *arrow* indicates the c.211delC mutation, shown in **c**. The *arrow* shows the deletion of C at nucleotide position 211 of the *KCNQ4* cDNA sequence. The deletion results in a frameshift after Gly70 (FS71), followed by 67 novel amino acids and a premature stop codon at amino acid position 138 (p.Q71fsX138)

Table 2 Clinical features of family members with c.211delC

Family members	Age	Onset (years)	Sex	Hearing threshold (dB)										Age at the test
				500 Hz		1,000 Hz		2,000 Hz		4,000 Hz		8,000 Hz		
				Right	Left	Right	Left	Right	Left	Right	Left	Right	Left	
II-5	78	22	Male	50	40	75	65	85	>95	>95	>95	>95	>95	71
II-7	71	8	Male	85	85	>95	>95	>95	>95	>95	>95	>95	>95	64
II-9	69	50	Female	30	40	40	35	>95	>95	>95	>95	>95	>95	62
II-11	64	N/A	Female	25	20	30	35	85	75	>90	>90	>90	>90	58
III-3	48	20	Male	10	20	30	25	75	80	>95	>95	>95	>95	41
III-5	52	30	Male	30	20	30	40	80	80	>95	90	>95	>95	45
III-8	51	N/A	Male	20	10	10	10	80	>90	>90	>90	>90	>90	45
III-12	34	N/A	Female	10	15	15	10	15	20	60	60	80	70	34
III-13	46	N/A	Female	N/A	N/A	N/A	N/A	N/A	N/A	N/A	N/A	N/A	N/A	N/A
IV-2	23	17	Female	15	15	5	10	10	15	45	45	65	65	18
IV-3	21	14	Male	10	5	10	10	40	45	70	60	85	70	20
IV-4	18	15	Male	15	15	10	10	40	30	50	45	65	65	18
IV-5	20	15	Male	10	10	10	10	10	10	10	10	30	20	15

N/A No information was available

ment in this family was progressive, starting with high frequencies and including middle and low frequencies later in life. According to the anamnestic data, the age at onset varied from 8–50 years.

Discussion

We have identified a novel *KCNQ4* mutation in a large Japanese pedigree with hearing loss by a genome-wide linkage analysis followed by the mutational analysis of candidate genes. The identified mutation was a one-base deletion in exon 1 of the *KCNQ4* gene, c.211delC, which caused a profoundly truncated peptide without the transmembrane portion of the potassium channel (p.Q71fsX138). Individuals with the apparently null mutation c.211delC had late-onset and pure high-frequency hearing loss, which did not resemble the phenotypes of the patients with the *KCNQ4* missense mutations. The individuals with c.211delC had phenotypes similar to those of patients with the c.211_223del (Topsakal et al. 2005). Dominant-negative mechanism has been suggested to underlie the pathogenesis of hearing loss caused by the missense *KCNQ4* mutations. Concordance of the mild phenotypes in two different null mutations, c.211_223del and c.211delC, suggests the genotype–phenotype correlation in which *KCNQ4* deletions are associated with later-onset and milder hearing loss than the missense mutations.

The phenotypic difference may be caused by the difference in the pathogenic mechanism. Two null mutations (c.211_223del and c.211delC) are expected to yield a KCNQ4 protein that is truncated before the first transmembrane region. Although deleterious mutations result in haploinsufficiency, the function of normal KCNQ4 protein produced from the intact allele may be spared. Fifty-percent decrease in normal KCNQ4 channels may lead to mild hearing impairment. Haploinsufficiency has been suggested to underlie the pathogenesis of both long QT syndrome and benign familial neonatal convulsions caused by *KCNQ1* and *KCNQ2* or *KCNQ3* mutations, respectively (Gouas et al. 2004; Rogawski 2000). In contrast, the dominant-negative effect due to missense mutations significantly interferes with the normal channel subunit. Six missense mutations have been identified in the KCNQ4 gene to date. Five mutations are located in the *KCNQ4* P-loop domain, and one mutation is located in the sixth transmembrane domain. Because these missense mutations are located in the critical domain of the protein, they may cause the dominant-negative effect.

The LOD score estimated at the early stage of this study was 3.0, which was far lower than the final estimation. The NPL score at the early stage was estimated to be 8.0, suggesting the possibility of incomplete penetrance. The identified *KCNQ4* mutation, c.211delC, was also present in a family member III-12, who had been classified as an unaffected individual. She did not complain of any difficulty in hearing. After the identification of the causative mutation we performed the audiological examination on her. It turned out that she had mild hearing impairment only in high-frequency, in concordance with her genotype. Re-analysis using this information showed an LOD score of 5.42. Thus, the deafness caused by the c.211delC appeared to be transmitted at a level of complete penetrance. The current study illustrates the potential difficulty of linkage analysis in slowly progressive hearing loss in a limited frequency range. Thorough otological examinations may be required even in individuals who are seemingly not affected upon interview.

Although more than 30 deafness genes have been so far identified, the genotype–phenotype relation in each allelic mutation remains largely unidentified. Elucidation of the genotype–phenotype correlations would facilitate informative genetic counseling.

Acknowledgements We are grateful to the family members for participating in this study. We thank Ms. Ikuko Sato and Ms. Yasuko Murayama for excellent technical assistance. This work was supported by Grants-in-Aid for Scientific Research from the Ministry of Education, Culture, Sports, Science and Technology, Japan, and grants from the Ministry of Health, Labor, and Welfare, Japan.

References

Akita J, Abe S, Shinkawa H, Kimberling WJ, Usami S (2001) Clinical and genetic features of nonsyndromic autosomal dominant sensorineural hearing loss: KCNQ4 is a gene responsible in Japanese. J Hum Genet 46:355–361

Coucke P, Van Camp G, Djoyodiharjo B, Smith SD, Frants RR, Padberg GW, Darby JK, Huizing EH, Cremers CW, Kimberling WJ et al (1994) Linkage of autosomal dominant hearing loss to the short arm of chromosome 1 in two families. N Engl J Med 331:425–431

Coucke PJ, Van Hauwe P, Kelley PM, Kunst H, Schatteman I, Van Velzen D, Meyers J, Ensink RJ, Verstreken M, Declau F, Marres H, Kastury K, Bhasin S, McGuirt WT, Smith RJ, Cremers CW, Van de Heyning P, Willems PJ, Smith SD, Van Camp G (1999) Mutations in the KCNQ4 gene are responsible for autosomal dominant deafness in four DFNA2 families. Hum Mol Genet 8:1321–1328

Gouas L, Bellocq C, Berthet M, Potet F, Demolombe S, Forhan A, Lescasse R, Simon F, Balkau B, Denjoy I, Hainque B, Baro I, Guicheney P (2004) New KCNQ1 mutations leading to haploinsufficiency in a general population: defective trafficking of a KvLQT1 mutant. Cardiovasc Res 63:60–68

Kenneson A, Van Naarden Braun K, Boyle C (2002) GJB2 (connexin 26) variants and nonsyndromic sensorineural hearing loss: a HuGE review. Genet Med 4:258–274

Kruglyak L, Daly MJ, Reeve-Daly MP, Lander ES (1996) Parametric and nonparametric linkage analysis: a unified multipoint approach. Am J Hum Genet 58:1347–1363

Kubisch C, Schroeder BC, Friedrich T, Lutjohann B, El-Amraoui A, Marlin S, Petit C, Jentsch TJ (1999) KCNQ4, a novel potassium channel expressed in sensory outer hair cells, is mutated in dominant deafness. Cell 96:437–446

Kudo T, Ikeda K, Kure S, Matsubara Y, Oshima T, Watanabe K, Kawase T, Narisawa K, Takasaka T (2000) Novel mutations in the connexin 26 gene (GJB2) responsible for childhood deafness in the Japanese population. Am J Med Genet 90:141–145

Kudo T, Kure S, Ikeda K, Xia AP, Katori Y, Suzuki M, Kojima K, Ichinohe A, Suzuki Y, Aoki Y, Kobayashi T, Matsubara Y (2003) Transgenic expression of a dominant-negative connex-

in26 causes degeneration of the organ of Corti and non-syndromic deafness. Hum Mol Genet 12:995–1004
Lathrop GM, Lalouel JM, Julier C, Ott J (1984) Strategies for multilocus linkage analysis in humans. Proc Natl Acad Sci USA 81:3443–3446
Marazita ML, Ploughman LM, Rawlings B, Remington E, Arnos KS, Nance WE (1993) Genetic epidemiological studies of early-onset deafness in the U.S. school-age population. Am J Med Genet 46:486–491
Morton NE (1991) Genetic epidemiology of hearing impairment. Ann N Y Acad Sci 630:16–31
Richard G, White TW, Smith LE, Bailey RA, Compton JG, Paul DL, Bale SJ (1998) Functional defects of Cx26 resulting from a heterozygous missense mutation in a family with dominant deaf-mutism and palmoplantar keratoderma. Hum Genet 103:393–399
Rogawski MA (2000) KCNQ2/KCNQ3 K+ channels and the molecular pathogenesis of epilepsy: implications for therapy. Trends Neurosci 23:393–398
Talebizadeh Z, Kelley PM, Askew JW, Beisel KW, Smith SD (1999) Novel mutation in the KCNQ4 gene in a large kindred with dominant progressive hearing loss. Hum Mutat 14:493–501
Topsakal V, Pennings RJ, te Brinke H, Hamel B, Huygen PL, Kremer H, Cremers CW (2005) Phenotype determination guides swift genotyping of a DFNA2/KCNQ4 family with a hot spot mutation (W276S). Otol Neurotol 26:52–58
Usami S, Koda E, Tsukamoto K, Otsuka A, Yuge I, Asamura K, Abe S, Akita J, Namba A (2002) Molecular diagnosis of deafness: impact of gene identification. Audiol Neurotol 7:185–190
Van Camp G, Coucke PJ, Kunst H, Schatteman I, Van Velzen D, Marres H, van Ewijk M, Declau F, Van Hauwe P, Meyers J, Kenyon J, Smith SD, Smith RJ, Djelantik B, Cremers CW, Van de Heyning PH, Willems PJ (1997) Linkage analysis of progressive hearing loss in five extended families maps the DFNA2 gene to a 1.25-Mb region on chromosome 1p. Genomics 41:70–74
Van Camp G, Coucke PJ, Akita J, Fransen E, Abe S, De Leenheer EM, Huygen PL, Cremers CW, Usami S (2002) A mutational hot spot in the KCNQ4 gene responsible for autosomal dominant hearing impairment. Hum Mutat 20:15–19
Van Hauwe P, Coucke PJ, Ensink RJ, Huygen P, Cremers CW, Van Camp G (2000) Mutations in the KCNQ4 K+ channel gene, responsible for autosomal dominant hearing loss, cluster in the channel pore region. Am J Med Genet 93:184–187
Xia JH, Liu CY, Tang BS, Pan Q, Huang L, Dai HP, Zhang BR, Xie W, Hu DX, Zheng D, Shi XL, Wang DA, Xia K, Yu KP, Liao XD, Feng Y, Yang YF, Xiao JY, Xie DH, Huang JZ (1998) Mutations in the gene encoding gap junction protein beta-3 associated with autosomal dominant hearing impairment. Nat Genet 20:370–373

HUMAN MUTATION 27(4), 343–352, 2006

RESEARCH ARTICLE

Comprehensive Mutation Analysis of *GLDC*, *AMT*, and *GCSH* in Nonketotic Hyperglycinemia

Shigeo Kure,[1]* Kumi Kato,[1,10] Agirios Dinopoulos,[2] Chuck Gail,[2] Ton J. deGrauw,[2] John Christodoulou,[3] Vladimir Bzduch,[4] Rozalia Kalmanchey,[5] Gyorgy Fekete,[5] Alex Trojovsky,[6] Barbara Plecko,[7] Galen Breningstall,[8] Jun Tohyama,[9] Yoko Aoki,[1] and Yoichi Matsubara[1,10]

[1]*Department of Medical Genetics, Tohoku University School of Medicine, Sendai, Japan;* [2]*Division of Pediatric Neurology, Cincinnati Children's Hospital, Cincinnati, Ohio;* [3]*Discipline of Paediatrics and Child Health, University of Sydney and Royal Alexandra Hospital for Children, Westmead, Australia;* [4]*First Department of Pediatrics, Comenius University Children's Hospital, Bratislava, Slovakia;* [5]*Department of Pediatrics, Semmelweis University, Budapest, Hungary;* [6]*Institute for Medical Biology and Human Genetics, Medical University of Graz, Graz, Austria;* [7]*Department for Pediatrics, Medical University of Graz, Graz, Austria;* [8]*Department of Pediatrics (Neurology); Park Nicollet Clinic, Minneapolis, Minnesota;* [9]*Department of Pediatrics, Nishi-Niigata Chuo National Hospital, Niigata, Japan;* [10]*21st COE Program "Comprehensive Research and Education Center for Planning of Drug Development and Clinical Evaluation," Tohoku University, Sendai, Japan*

Communicated by Jan P. Kraus

Nonketotic hyperglycinemia (NKH) is an inborn error of metabolism characterized by accumulation of glycine in body fluids and various neurological symptoms. NKH is caused by deficiency of the glycine cleavage multi-enzyme system with three specific components encoded by *GLDC*, *AMT*, and *GCSH*. We undertook the first comprehensive screening for *GLDC*, *AMT*, and *GCSH* mutations in 69 families (56, six, and seven families with neonatal, infantile, and late-onset type NKH, respectively). *GLDC* or *AMT* mutations were identified in 75% of neonatal and 83% of infantile families, but not in late-onset type NKH. No *GCSH* mutation was identified in this study. *GLDC* mutations were identified in 36 families, and *AMT* mutations were detected in 11 families. In 16 of the 36 families with *GLDC* mutations, mutations were identified in only one allele despite sequencing of the entire coding regions. The *GLDC* gene consists of 25 exons. Seven of the 32 *GLDC* missense mutations were clustered in exon 19, which encodes the cofactor-binding site Lys754. A large deletion involving exon 1 of the GLDC gene was found in Caucasian, Oriental, and black families. Multiple origins of the exon 1 deletion were suggested by haplotype analysis with four *GLDC* polymorphisms. This study provides a comprehensive picture of the genetic background of NKH as it is known to date. Hum Mutat 27(4), 343–352, 2006. © 2006 Wiley-Liss, Inc.

KEY WORDS: GLDC; AMT; GCSH; glycine encephalopathy; nonketotic hyperglycinemia; NKH; glycine cleavage system; mutation spectrum; genotype–phenotype

INTRODUCTION

Nonketotic hyperglycinemia (NKH, MIM# 605899), also termed glycine encephalopathy, is an inborn error of amino acid metabolism characterized by the accumulation of a large amount of glycine in body fluids [Hamosh and Johnston, 2001]. Glycine levels are elevated to a much greater extent in cerebrospinal fluid (CSF) than in plasma; hence, an abnormally high value for the CSF/plasma glycine ratio is observed. NKH is clinically classified (by onset of symptoms) as three types: neonatal, infantile, or late-onset. Later onset appears to be associated with a better prognosis. The vast majority of patients fall into the neonatal category, which involves a stereotypic presentation with severe hypotonia, apnea requiring assisted ventilation, and intractable seizures. Approximately 30% of such patients die in the neonatal period. Survivors often have severe psychomotor retardation, although 15–20% of survivors achieve developmental milestones such as head control, independent sitting, or walking [Hoover-Fong et al., 2004]. Patients with the infantile type of NKH are often asymptomatic in the neonatal period and the phenotype is characterized by mild to moderate psychomotor retardation, behavioral problems, seizures, and chorea. The clinical presentations of late-onset NKH are heterogeneous. In previous studies, two families did not have seizures or mental retardation, but exhibited progressive paraplegia and optic atrophy [Bank and Morrow, 1972; Steiman et al., 1979]. Another family was reported to present with mental retardation and choreoathetosis [Singer et al., 1989].

The fundamental defect lies in the glycine cleavage system (GCS; EC2.1.2.10) [Tada et al., 1969]. The GCS is a mitochondrial complex enzyme system that consists of four

The Supplementary Material referred to in this article can be accessed at http://www.interscience.wiley.com/jpages/1059-7794/suppmat.

Received 11 July 2005; accepted revised manuscript 9 November 2005.

*Correspondence to: Shigeo Kure, M.D., Department of Medical Genetics, Tohoku University School of Medicine, 1-1 Seiryomachi, Aobaku, Sendai 980-8574, Japan.
E-mail: skure@mail.tains.tohoku.ac.jp

Grant sponsor: Ministry of Education, Culture, Sports, Science, and Technology; Ministry of Health, Labor, and Public Welfare in Japan.
DOI 10.1002/humu.20293
Published online 31 January 2006 in Wiley InterScience (www.interscience.wiley.com).

individual proteins [Kikuchi, 1973]: glycine decarboxylase (also called P-protein), aminomethyltransferase (T-protein), hydrogen carrier protein (H-protein), and dihydrolipoamide dehydrogenase (L-protein). The enzymatic analysis of NKH patients revealed that approximately 80% of patients with NKH have a *GLDC* deficiency and the rest have an *AMT* deficiency [Tada and Hayasaka, 1987]. Mitochondrial precursors of human P, T, H, and L-proteins consist of 1,020, 403, 173, and 509 amino acids, respectively. Dihydrolipoamide dehydrogenase is a housekeeping enzyme that serves as an E3 component of other α-keto acid dehydrogenase complexes, such as pyruvate dehydrogenase. Deficiency of dihydrolipoamide dehydrogenase causes progressive neurological deterioration with lactic acidosis but not hyperglycinemia [Hong et al., 1996]. The three GCS-specific components (P, T, and H-proteins) are encoded by distinct genes: *GLDC* (MIM# 238300) on chromosome 9p24 [Isobe et al., 1994], *AMT* on 3p21.1-21.2 [Nanao et al., 1994], and *GCSH* (MIM# 238330) on 16p24 [Kure et al., 2001], respectively.

To date, a limited number of NKH mutations have been reported (Human Gene Mutation Database, Cardiff; http://www.hgmd.cf.ac.uk). The *GLDC* mutations reported to date include the S564I mutation that is prevalent in Finnish patients [Kure et al., 1992], the R515S mutation found in 5% of Caucasian patients [Toone et al., 2000], microdeletions [Kure et al., 1991], large deletions [Takayanagi et al., 2000; Sellner et al., 2005], one abnormal splicing [Flusser et al., 2005], one nonsense mutation [Sellner et al., 2005], and 10 missense mutations [Toone et al., 2002; Korman et al., 2004; Kure et al., 2004; Boneh et al., 2005; Dinopoulos et al., 2005]. The *AMT* gene (MIM# 238310) mutations identified to date include nine missense mutations [Nanao et al., 1994, 1994a; Kure et al., 1998; Toone et al., 2000, 2001, 2003], one microdeletion [Kure et al., 1998, 1998b], and one splicing mutation [Toone et al., 2000]. In *GCSH* we have found one abnormal splicing in a patient with a transient form of NKH [Kure et al., 2002]. Since multiple genes are responsible for NKH, previous studies screened only a small number of *GLDC* and *AMT* exons and/or a few patients, which hampered elucidation of the genetic background of NKH.

The purpose of the present study was to establish the mutation spectrum of NKH by performing a comprehensive screening for mutations in *GLDC*, *AMT*, and *GCSH* in 69 families with three different types of NKH. The structure of *AMT* has been determined [Nanao et al., 1994, 1994b]. Also, we previously reported the exon-intron organizations of *GLDC* [Takayanagi et al., 2000] and *GCSH* [Kure et al., 2001], which provided us with basic information to amplify the entire coding regions for the three genes. To increase the sensitivity of mutational screening, we directly sequenced all amplicons without employing prescreening scanning methods such as single-strand conformation polymorphism.

MATERIALS AND METHODS

Patients

Patients were examined in the metabolic disease clinics of a number of referring hospitals. NKH was clinically suspected based on the presentation of symptoms characteristic of each disease type and electroencephalograms (EEG) recordings, and were subsequently confirmed by amino acid analysis. The CSF/serum glycine ratio at diagnosis was >0.04 in all patients, whereas it was <0.03 in normal neonates. Patients were classified into three clinical subtypes (neonatal, infantile, and late-onset) based on the onset of clinical symptoms.

Neonatal type. We studied 56 families with neonatal onset. Initial symptoms, including hypotonia, apnea, and coma, developed within 7 days after birth–in most cases within 3 days. Almost all of the patients showed a burst suppression pattern on EEG within 2 weeks after birth, and hypsarrhythmia thereafter.

Infantile type. Six families were enrolled. Symptoms started at 3–12 months of age. Five of the six patients had no symptoms in the neonatal period. Very mild hypotonia and apnea were observed in patient P107 [Dinopoulos et al., 2005]. Mild mental retardation and abnormal behaviors, such as aggressiveness, developed in adolescence.

Late-onset type. We studied seven patients with late-onset NKH. All seven patients had elevated glycine concentrations in repeated amino acid analysis of CSF and/or plasma. Spastic paraplegia without mental retardation developed in three of the seven patients. These patients resembled those in previously reported families [Bank and Morrow, 1972; Steiman et al., 1979]. The rest of the patients presented with mental retardation after they entered school or during adolescence. There is some confusion in terms of phenotypic classification of the mild form of the infantile type and the late-onset type, since there are some reports of patients in whom developmental delay or mild hypotonia started in the middle or late infantile periods [Flannery et al., 1983; Singer et al., 1989]. We classified such patients as having the infantile type—not the late-onset type. In the present study we classified patients as having the late-onset type when they were free of any symptoms during infancy.

Mutational Screening

Exons and flanking intron sequences of *GLDC* (GenBank NM_000170, NT_008413.16), *AMT* (GenBank NM_00481, NT_086638.1), and *GCSH* (GenBank NM_004483, NC_00016.8) were amplified by PCR from genomic DNA, followed by direct sequencing analysis using the dye-primer sequencing method as previously described [Kure et al., 2001]. The 18-mer oligonucleotides of the M13 and reverse sequencing primers were added to the 5′ end of the forward and reverse PCR primers, respectively. We initially screened for a large deletion involving *GLDC* exon 1 by semiquantitative PCR using the pseudogene of *GLDC* (*GLDCP*) as a gene dose control [Takayanagi et al., 2000]. PCR primer sequences for amplifying *GLDC* exons 1–6 were previously reported [Takayanagi et al., 2000], and those for other exons are described in Supplementary Table S1 (available online at http://www.interscience.wiley.com/jpages/1059-7794/suppmat). Each PCR cycle consisted of denaturing at 98°C for 10 sec, annealing at 55°C for 30 sec, and extension at 72°C for 30 sec, with repetition for 35 cycles. For PCR amplification of *GLDC* exon 1, 10% dimethylformamide was added to the reaction mixture. Fifty control subjects were subsequently screened for any detected base changes to exclude noncausative polymorphisms. If no mutations were detected in the sequencing analysis of *GLDC*, we screened for mutations in *AMT* by amplifying all of the nine exons. When no mutations were identified in either *GLDC* or *AMT*, we sequenced all of the five exons in *GCSH*. For characterization of *GLDC* and *AMT* missense mutations, each mutated amino acid residue was compared with the corresponding amino acid in rat [Sakata et al., 2001], chicken [Kume et al., 1991], pea [Turner et al., 1992], and *E. coli* [Okamura-Ikeda et al., 1993], as shown in Tables 2 and 3.

Characterization of the *GLDC* Deletion

We identified the minimum deleted region of both alleles of each homozygous patient of the *GLDC* exon 1 deletion. Fifteen sequence tagged sites (STSs) were used for this deletion mapping,

as illustrated in Fig. 1. PCR primer sequences and amplification conditions for D9S281 and RH92434 were obtained from the website of the UCSC Genome Browser (http://genome.ucsc.edu). The PCR primer sequences and amplicon sizes of STSs 1–8 are presented in Supplementary Table S1. STSs 1–7 were located 5′ upstream of the *GLDC* gene, and STS 8 was located in intron 2. Amplification primers for *GLDC* exons 1–5 were also used in the deletion mapping. We amplified these 15 STSs by using genomic DNA of Patients P5 and P36 as a template in order to test whether each STS was involved in the homozygously deleted region. Structural information about the 5′ upstream region of *GLDC* and the location of *Alu* motifs was obtained from the UCSC Genome Browser (Fig. 1).

RESULTS

Mutation Screening

We performed mutational screening in 69 NKH families (56 neonatal type, six infantile type, and seven late-onset type). First, the *GLDC* exon 1 deletion was screened by semiquantitative PCR amplification using the *GLDCP* as a control of the gene copy number. This deletion was found in six families (Table 1). Subsequent extensive sequencing of *GLDC*, *AMT*, and *GCSH* coding exons revealed that 42 of the 56 neonatal-type families (75%) had *GLDC* or *AMT* mutations in at least one of two alleles. *GLDC* mutations were found in 31 (74%) and *AMT* mutations were detected in 11 (26%) of the 42 families. No differences were

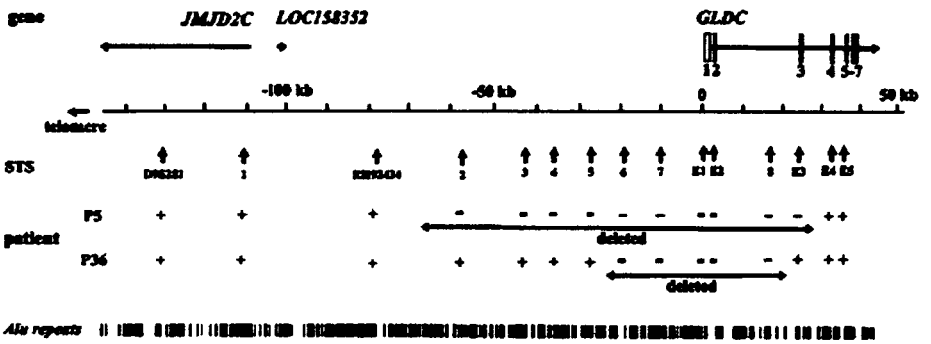

FIGURE 1. **Mapping of the *GLDC* deletions. Genomic regions that were homozygously deleted in patients P5 and P36 were defined by amplification of 13 STS markers. The JMJD2C gene and the gene-like structure, LOC158352, are shown based on the information of the UCSC Genome Browser. E1–5 indicate amplicons including the *GLDC* exons 1–5, respectively. Amplicons (+) indicate that the STS was successfully amplified, while (–) means that the STS failed to be amplified.**

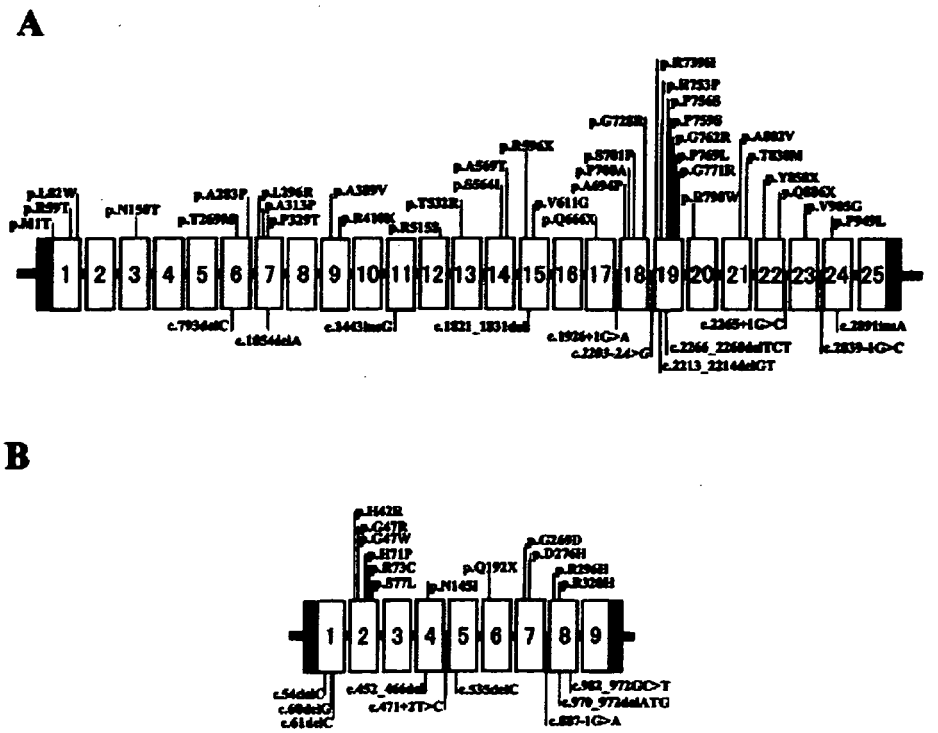

FIGURE 2. **NKH mutations identified in this and previous studies. The *GLDC* (A) and *AMT* (B) exons are indicated by open boxes, and noncoding regions are shaded. Missense and nonsense mutations are shown above the exon boxes, and deletions/insertions and mutations of splicing errors are indicated below the exon boxes.**

TABLE 1. Patients With *GLDC* or *AMT* Mutations

Family number	Ethnicity	Age of onset	Consanguinity	CSF Gly (mM)	CSF/serum Gly ratio	Mutation[a] Gene	Mutation 1	Mutation 2	Reference
Neonatal type									
P14	Caucasian	Day 1	No	296	0.25	*GLDC*	Exon 1 deletion	c.2714T>G	This study
P21	Caucasian	Day 1	Yes	71	0.24	*AMT*	c.230C>T	c.230C>T	This study
P26	Caucasian	Day 1	Yes	86	0.27	*AMT*	c.125A>G	c.125A>G	Kure et al. [1998a]
P29	Caucasian	Day 1	No	43	0.04	*GLDC*	c.793delC	ND	This study
P31	Caucasian	Day 1	No	196	0.26	*AMT*	c.471+2T>C	c.887G>A	This study
P32	Caucasian	Day 1	No	32	0.20	*GLDC*	c.1786C>T	c.1786C>T	This study
P36	Caucasian	Day 1	No	220	0.18	*GLDC*	Exon 1 deletion	Exon 1 deletion	This study
P39	Caucasian	Day 1	No	187	0.13	*GLDC*	c.1595C>G	c.1832T>G	This study
P48	Caucasian	Day 1	No	198	0.20	*GLDC*	c.2665+1G>C	ND	This study
P49	Caucasian	Day 1	No	213	0.17	*GLDC*	c.2203–2A>G	ND	This study
P59	Caucasian	Day 1	Yes	202	0.23	*GLDC*	c.1996C>T	c.1996C>T	This study
P5	Oriental	Day 1	No	240	0.18	*GLDC*	Exon 1 deletion	Exon 1 deletion	Ohya et al. [1991]
P6	Oriental	Day 1	No	160	0.09	*GLDC*	c.245T>G	c.1821_18311del	Kure et al. [2004]
P19	Oriental	Day 1	No	264	0.30	*GLDC*	c.449A>C	c.2368C>T	Kure et al. [2004]
P25	Oriental	Day 1	No	74	0.34	*AMT*	c.54delC	c.826G>C	Kure et al. [1998b]
P74	Oriental	Day 1	No	117	0.12	*GLDC*	c.2311G>A	ND	This study
P86	Oriental	Day 1	No	177	0.20	*GLDC*	c.2213_2214delGT	ND	This study
P93	Oriental	Day 1	No	130	0.13	*GLDC*	c.2105C>T	ND	This study
P115	Oriental	Day 1	No	145	0.11	*AMT*	c.147delG	c.970_972delATG	This study
P124	Oriental	Day 1	No	300	0.11	*GLDC*	c.255+1G>A	c.806C>T	This study
P30	Caucasian	Day 2	No	121	0.19	*AMT*	c.60delG	c.471+2T>C	This study
P44	Caucasian	Day 2	No	98	0.11	*GLDC*	c.806C>T	c.255+1G>A	This study
P46	Caucasian	Day 2	No	155	0.13	*GLDC*	c.2293C>T	c.1705G>A	This study
P47	Caucasian	Day 2	No	78	0.17	*GLDC*	c.2519T>A	ND	This study
P61	Caucasian	Day 2	No	186	0.17	*AMT*	c.982_972GC>T	c.452_466del	This study
P75	Caucasian	Day 2	No	167	0.16	*AMT*	c.212A>C	c.217C>T	This study
P3	Oriental	Day 2	No	151	0.10	*GLDC*	c.2306C>T	c.2846C>T	This study
P4	Oriental	Day 2	No	387	0.28	*GLDC*	c.2258A>C	c.2839–1G>C	This study
P7	Oriental	Day 2	No	164	0.10	*GLDC*	c.2266_2268delTTC	ND	Kure et al. [1991]
P8	Oriental	Day 2	No	209	0.31	*GLDC*	c.2080G>C	ND	This study
P10	Oriental	Day 2	No	517	0.20	*GLDC*	c.887T>G	ND	This study
P77	Oriental	Day 2	No	148	0.12	*GLDC*	c.449A>C	c.1926+1G>A	This study
P91	Oriental	Day 2	No	132	0.08	*AMT*	c.61delC	c.535delC	This study
P69	Oriental	Day 3	No	220	0.12	*GLDC*	c.2311G>A	ND	This study
P70	Oriental	Day 3	No	68	0.19	*GLDC*	Exon 1 deletion	ND	This study
P120	Oriental	Day 3	No	324	0.19	*GLDC*	c.2574T>G	ND	This study
P23	Oriental	Day 4	No	83	0.14	*GLDC*	c.2182G>C	ND	This study
P104	Caucasian	Day 4	No	240	0.26	*GLDC*	c.1166C>T	c.1443insG	This study
P15	Black	Day 5	No	333	0.08	*GLDC*	Exon 1 deletion	c.2891insA	This study
P34	Caucasian	Day 6	No	174	0.08	*AMT*	c.139G>T	ND	This study
P76	Caucasian	Day 6	No	215	0.18	*AMT*	c.136G>A	c.230C>T	This study
P72	Black	Day 7	No	117	0.20	*GLDC*	c.2665+1G>C	c.176G>C	This study
Infantile type									
P50	Caucasian	3 months	No	200	0.25	*GLDC*	Exon 1 deletion	c.2311G>A	This study
P78	Caucasian	6 months	No	46	0.06	*GLDC*	c.2216G>A	c.2216G>A	Dinopoulos et al. [2005]
P12	Caucasian	12 months	No	41	0.04	*GLDC*	c.2216G>A	ND	Christodoulou et al. [1993]
P107	Caucasian	Unclear[b]	No	150	0.09	*GLDC*	c.1166C>T	c.1166C>T	Dinopoulos et al. [2005]
P108	Caucasian	Unclear[b]	No	55	0.05	*GLDC*	c.1166C>T	c.1166C>T	Dinopoulos et al. [2005]

[a]DNA mutation numbering is based on cDNA sequence: +1 corresponds to the A of the ATG translation initiation codon. *GLDC*: NM_000170; *AMT*: NM_00481.
[b]Developmental delay in infantile period.
ND, not detected.

TABLE 2. *GLDC* Mutations*

Mutation	Location	Consequence of mutation	No. of families	Novel mutation	Comments				
Missense mutations					Evolutionary conservation				
					Human	Rat	Chicken	Pea	*E.coli*
c.176G>C	Exon 1	p.R59T	1	Yes	Arg	Arg	Arg	Ser	Ser
c.245T>G	Exon 1	p.L82W	1	No	Lue	Lue	Val	Val	Val
c.449A>C	Exon 3	p.N150T	2	No	Asn	Asn	Asn	Asn	Asn
c.806C>T	Exon 6	p.T269M	2	Yes	Thr	Thr	Thr	Thr	Thr
c.887T>G	Exon 7	p.L296R	1	Yes	Leu	Leu	Leu	Leu	Ile
c.1166C>T	Exon 9	p.A389V	3	No	Ala	Ala	Ala	Ala	Ala
c.1595C>G	Exon 13	p.T532R	1	Yes	Thr	Thr	Thr	His	Thr
c.1705G>A	Exon 14	p.A569T	1	Yes	Ala	Ala	Ala	Met	Ile
c.1832T>G	Exon 15	p.V611G	1	Yes	Val	Val	Ile	Phe	Val
c.2080G>C	Exon 18	p.A694P	1	Yes	Ala	Ala	Ala	Ala	Cys
c.2105C>T	Exon 18	p.S701F	1	Yes	Ser	Ser	Ser	Ser	Ser
c.2182G>C	Exon 18	p.G728R	1	Yes	Gly	Gly	Gly	Gly	Gly
c.2216G>A	Exon 19	p.R739H	2	No	Arg	Arg	Arg	Ser	Ser
c.2258A>C	Exon 19	p.H753P	1	Yes	His	His	His	His	His
c.2293C>T	Exon 19	p.P765S	1	Yes	Pro	Pro	Pro	Pro	Pro
c.2306C>T	Exon 19	p.P769L	1	Yes	Pro	Pro	Pro	Pro	Pro
c.2311G>A	Exon 19	p.G771R	3	Yes	Gly	Gly	Gly	Gly	Gly
c.2368C>T	Exon 20	p.R790W	1	No	Arg	Arg	–	–	–
c.2519T>A	Exon 21	p.M840K	1	Yes	Met	Met	Met	Met	Ile
c.2714T>G	Exon 23	p.V905G	1	Yes	Val	Val	Ile	Ile	Val
c.2846C>T	Exon 24	p.P949L	1	Yes	Pro	Pro	Pro	Pro	Pro
Nonsense mutations									
c.1786C>T	Exon 15	p.R596X	1	Yes					
c.1996C>T	Exon 17	p.Q666X	1	Yes					
c.2574T>G	Exon 22	p.Y858X	1	Yes					
Deletions and insertions									
Exon 1 deletion	Exon 1	Deletion including exon 1	6	No	A recurrent mutation				
c.793delC	Exon 6	Deletion of first letter of 265Gln codon	1	Yes	FS after codon 264/TRM at codon 296				
c.1821_1831del	Exon 15	11-bp deletion started at third letter of 607Gly codon	1	No	FS after codon 607/TRM at codon 669				
c.1443insG	Exon 11	Insertion of G after third letter of 481Leu codon	1	Yes	FS at codon 482/TRM at codon 491				
c.2213_2214delGT	Exon 19	Deletion of GT in 738Cys codon	1	Yes	FS after codon 738/TRM at codon 745				
c.2266_2268delTTC	Exon 19	Deletion of TTC in 756Phe codon	1	No	No FS/TRM at codon 1019				
c.2891insA	Exon 24	Insertion of A after second letter of 964Tyr codon	1	Yes	No FS/TRM at codon 964				
Aberrant splicing									
c.255+1G>A	Intron 2	Disruption of splicing donor site, gt>at	1	Yes					
c.1926+1G>A	Intron 17	Disruption of splicing donor site, gt>at	1	Yes					
c.2203–2A>G	Intron 18	Disruption of splicing acceptor site, ag>gg	1	Yes					
c.2665+1G>C	Intron 22	Disruption of splicing donor site, gt>ct	2	Yes					
c.2839–1G>C	Intron 23	Disruption of splicing acceptor site, ag>cg	1	Yes					

*DNA mutation numbering is based on cDNA sequence: +1 corresponds to the A of the ATG translation initiation codon. *GDLC*: NM_000170. FS, frameshift; TRM, termination codon.

observed in CSF glycine levels between 42 mutation-positive and 14 mutation-negative individuals. *GLDC* mutations were detected in five (83%) of the six patients with infantile NKH. No mutations were found in *GLDC*, *AMT*, or *GCSH* in any of seven patients with late-onset NKH. NKH mutations were highly heterogeneous. Only nine of the 47 mutation-positive individuals were homozygous for a single mutation (three individuals from consanguineous families (P21, P26, and P59), and five homozygotes of recurrent mutations (P36, P5, P78, P107, and P108)). Patient P32 was homozygous for a private mutation (p.R596X), even though there was no evidence that he was the product of a consanguineous marriage. No *GCSH* mutations were identified in this study.

TABLE 3. *AMT* Mutations*

Mutation	Location	Sequence alternation	No. of families	Novel mutation	Comments				
Missense mutations					Evolutionary Conservation				
					Human	Rat	Chicken	Pea	*E.coli*
c.125A>G	Exon 2	p.H42R	1	No	His	His	His	His	His
c.136G>A	Exon 2	p.G47R	1	Yes	Gly	Gly	Gly	Gly	Ala
c.139G>T	Exon 2	p.G47W	1	Yes	Gly	Gly	Gly	Gly	Ala
c.212A>C	Exon 2	p.H71P	1	Yes	His	His	His	Asn	Ala
c.217C>T	Exon 2	p.R73C	1	Yes	Arg	Arg	Arg	Arg	Arg
c.230C>T	Exon 2	p.S77L	1	Yes	Ser	Ser	Ser	Ser	Gly
c.826G>C	Exon 7	p.D276H	1	No	Asp	Asp	Asp	Asp	Glu
c.887G>A	Exon 8	p.R296H	1	No	Arg	Arg	Lys	Arg	Lys
Deletions and insertion									
c.54delC	Exon 1	Deletion of third letter of 18Phe codon	1	No	FS at codon 20/TRM at codon 95				
c.60delG	Exon 1	Deletion of third letter of 20Pro codon	1	Yes	FS at codon 21/TRM at codon 95				
c.61delC	Exon 1	Deletion of first letter of 21Ala codon	1	Yes	FS at codon 21/TRM at codon 95				
c.147delG	Exon 2	Deletion of third letter of 49Met codon	1	Yes	FS at codon 50/TRM at codon 95				
c.452_466del	Exon 4	Deletion start at second letter of 151Lys codon	1	Yes	No FS/TRM at codon 398				
c.535delC	Exon 5	Deletion of first letter of 179Leu codon	1	Yes	FS at codon 179/TRM at codon 180				
c.970_972delATG	Exon 8	Deleion of 320Met codon	1	Yes	No FS/TRM at codon 482				
c.982_972GC>T	Exon 8	GC in 328Ala codon was substitued byT	1	Yes	FS at codon 328/TRM at codon 337				
Aberrant splicing									
c.471+2T>C	Intron 4	Disruption of splicing donor site, gt>gc	2	Yes					

*DNA mutation numbering is based on cDNA sequence: +1 corresponds to the A of the ATG translation initiation codon. *AMT*: NM_00481.
FS, frameshift; TRM, termination codon.

GLDC Mutations

Deletion of exon 1 was detected in six patients (four Caucasian, one oriental, and one black). In this study we identified 36 *GLDC* mutations, 28 of which were novel (Table 2). None of the identified mutations were detected in 100 control alleles. There were 21 missense mutations, three nonsense mutations, seven deletion/insertion mutations, and five splicing mutations Table 3. For all of the 21 missense mutations the substituted amino acids are conserved in rats, and 13 of the 21 amino acids are conserved from humans to *E. coli*. Such a high degree of evolutionary conservation presumably reflects the functional importance of each of these amino acids. Seven mutations were found in multiple individuals with no apparent relationship. A missense mutation p.N150T was identified in oriental families, while p.T269M, p.A389V, p.R739H, and c.2665+1G>C were found in Caucasian families. Sequencing analysis of the *GLDC* gene revealed the presence of several polymorphisms, which were also found in control subjects (Table 4). Five of the polymorphisms were found in at least 10% of the control alleles tested. Three of them were found within exons (exon 1: c.249G>A; exon 4, c.501G>A; and exon 25, c.3070C>G (3′ noncoding region)). Two of them were located in introns (intron 9, c.1262+36A>G; and intron 19, c.2203-6insA). The c.2203-6insA polymorphism was located at the intron 19/exon 20 boundary, and substitutes the ttaaaaaaaa-tacag/GAAGAAA (A8 allele) to the ttaaaaaaaatacag/GAA GAAA (A9 allele). Other polymorphisms that were less frequently observed were c.438G>A (p.T146T) in exon 3, c.1261+36A>G (intron 9), and c.1261+52G>A (intron 9).

AMT Mutations

A total of 17 mutations (including 13 novel mutations) were identified, including eight missense mutations, eight deletion/insertion mutations, and one splicing mutation. The evolutionary conservation of each mutated amino acid is shown in Table 3. All of these amino acids are conserved among humans, rats, and chickens, and six of eight amino acids are also conserved in peas, which suggests that they are functionally important. All of the deletion/insertion mutations generated a profoundly truncated AMT polypeptide. Two polymorphic sites were observed in two AMT exons: exon 2, c.327T>C; and exon 8, c.1083G>A.

Characterization of the *GLDC* Exon 1 Deletion

To define the boundaries of the exon 1 deletions, eight STSs were designed: seven STSs at the region 150 kb upstream of *GLDC*, and one STS in intron 2 of *GLDC* (Fig. 1; Supplementary Table S1). Two additional published STSs (D9S281 and RH92434) and *GLDC* exons 1–5 were also used for the deletion mapping. We amplified a total of 15 STSs using genomic DNA as the templates obtained from Patients P5 and P36, who were homozygous for the *GLDC* exon 1 deletion. In Patient P5, STSs 2–8 and exons 1–3 were not amplified, indicating that the 80–100 kb was homozygously deleted. In Patient P36, STSs 6–8, and exons 1–2 failed to be amplified, demonstrating a 35–45 kb homozygous deletion. Both deletions did not extend to a known gene 5′ adjacent to *GLDC*: jumonji domain containing protein2C (*JMJD2C*). *Alu* repeats in this region were identified using the UCSD Genome Browser (Fig. 1).

TABLE 4. Haplotype Analysis of the *GLDC* Allele With the Exon 1 Deletion

			Polymorphic site			
Patients	Ethnicity	Allele	Exon 4 c.501G>A[a]	Intron 9 c.1262+36A>G	Intron 19 c.2203–6insA	Exon 25 (3′ noncoding region) c.3070C>G
P5	Oriental	Allele 1	G	A	A8	C
		Allele 2	G	A	A8	C
P14	Caucasian	Allele 1	G	A	A8	C
P36	Caucasian	Allele 1	G	A	A8	C
		Allele 2	G	A	A9	C
P50	Caucasian	Allele 1	A	G	A9	C

[a]DNA mutation numbering is based on cDNA sequence: +1 corresponds to the A of the ATG translation initiation codon. *GDLC*: NM_000170.

Haplotype Analysis of the *GLDC* Mutations

The identification of five polymorphisms within *GLDC* allowed us to determine the haplotypes of the mutant alleles with the exon 1 deletion. Haplotypes of the deletion allele were identified in four families (P5, P14, P36, and P50), but could not be determined in two families (P15 and P86; Table 4). Four mutant alleles shared the same haplotype (G, A, A8, C), with the genotypes of four polymorphic sites being written as follows: (c.501G>A, c.1232+36A>G, c.2203-6ins A, c3070C>G). Two additional haplotypes, (G, A, A9, C) and (A, G, A9, C) were also found, suggesting multiple origins of the exon 1 deletion.

Mutation Spectra of the *GLDC* and *AMT* Genes

The *GLDC* mutations detected in this study, as well as those from previous reports, are illustrated in Fig. 2A. The most striking feature of the mutation distribution is the clustering of the missense mutations in exon 19. Seven of the 32 missense mutations (22%) were identified in exon 19. The distribution of the *AMT* mutations is shown in Fig. 2B. No obvious clustering of the mutations was found in this gene.

DISCUSSION

We undertook an extensive screening for *GLDC*, *AMT*, and *GCSH* mutations in a cohort of patients with NKH, and the results reveal a comprehensive picture of the mutation spectrum of NKH to date. In this study, 36 *GLDC* mutations and 17 *AMT* mutations were detected, including 28 novel *GLDC* and 13 novel *AMT* mutations. In total, 75% of neonatal and 83% of infantile patients were positive for *GLDC* or *AMT* mutations. Mutations in NKH patients were highly heterogeneous. Patients were found to be compound heterozygotes in 38 of 47 mutation-positive cases (81%). This is in sharp contrast with findings in countries with a high incidence of NKH, such as Finland [von Wendt et al., 1979] and Israel [Korman and Gutman, 2002]. In those countries there are common mutations and many homozygotes for each common mutation. A *GLDC* missense mutation (p.564I) has been identified in Finland [Kure et al., 1992], and a *GLDC* missense mutation (p.M1 T) and *AMT* missense mutation (p.H42R) have been found in Israel [Boneh et al., 2005; Flusser et al., 2005].

In 16 of 36 families (44%) with *GLDC* mutations, we were able to identify a mutation in only one of two mutant alleles despite extensive mutational screening of *GLDC*, *AMT*, and *GCSH*. Mutations may present in promoter regions or introns of the GLDC gene, or large deletions or duplications may exist. Deletion of *GLDC* exon 1 was detected in eight of the 36 families (22%) with GLDC mutations. The deletion was found in Caucasian, oriental, and black patients. Subsequent haplotype analysis suggested multiple origins of the deletion. There is a high-density repeat region of *Alu* motifs in the 5′ upstream region and the introns of *GLDC*, which are reported to trigger a homologous recombination between two *Alu* motifs and cause a large deletion (e.g., the C1-inhibitor gene, *C1-INH* [Stoppa-Lyonnet et al., 1991]; lysyl hydroxylase gene, *PLOD1* [Pousi et al., 1994]; and a MutL mismatch repair gene, *hMLH1* [Mauillon et al., 1996]). We therefore speculate that the deletions of *GLDC* exon 1 are caused by homologous recombination between *Alu* repeats. Recently, Sellner et al. [2005] reported a deletion of *GLDC* exons 2–15 that was flanked by *Alu* motifs. *Alu*-mediated homologous deletion may occur not only in the 5′ region of *GLDC*, but also in other regions of *GLDC*.

No mutations were detected in seven patients with late-onset NKH, despite intensive screening of the entire coding regions of *GLDC*, *AMT*, and *GCSH*, which suggests that gene(s) other than GCS genes may be responsible for late-onset NKH. Several reports have described hyperglycinemic patients with no evidence of neurological symptoms until 1 year of age [Bank and Morrow, 1972; Steiman et al., 1979; Lane et al., 1991, 1998; Wiltshire et al., 2000; Ellaway et al., 2001]. The diagnosis of NKH was not confirmed by mutational analysis in any of those patients. Patients with atypical GE tend to have a relatively modest elevation of serum and CSF glycine concentrations, which may be also caused by other genetic disorders or therapeutic agents [Korman and Gutman, 2002]. Vanishing white matter disease is a type of leukoencephalopathy with characteristic MRI findings that is commonly associated with mild elevation of CSF glycine concentration [van der Knaap et al., 1999]. This disorder might have been classified as a late-onset NKH if the responsible genes (*EIF2B5* and *EIF2B2*) had not been identified [Leegwater et al., 2001]. For a more accurate diagnosis and better understanding of late-onset NKH patients, genetic characterization is of paramount importance. There are several other proteins that are functionally related to the GCS reaction. Lipoylation of H-protein is catalyzed by lipolyltransferase. The gene encoding the enzyme would be a good candidate for NKH [Fujiwara et al., 1999]. Two types of glycine transporters, GlyT1 and GlyT2, have been identified [Zafra et al., 1997]. GlyT2 is located only in the brain stem and spinal cord, while GlyT1 is distributed in the brain, kidney, and liver, and the latter transporter may have a role in maintaining the glycine level in both CSF and plasma. Thus, the GlyT1 gene is another good candidate gene for NKH.

A mutation in at least one of two alleles was identified in 47 of 62 patients with neonatal or infantile type NKH, 36 of whom (77%) had *GLDC* mutations. The dominance of the *GLDC* mutations over *AMT* mutations is in agreement with previous

enzymatic studies [Tada and Hayasaka, 1987; Toone et al., 2000]. No *GCSH* mutations were identified in any of the three clinical subtypes of NKH, suggesting that *GCSH* mutations are extremely rare in NKH. We recently identified a heterozygous splicing mutation in *GCSH* in a Japanese family with a peculiar type of NKH–transient type NKH [Kure et al., 2002]. Transient NKH is indistinguishable from neonatal NKH in terms of the onset of disease, but serum and CSF glycine are normalized within 2–8 weeks [Luder et al., 1989; Schiffmann et al., 1989]. A girl with atypical NKH was reported to have low enzymatic activity of the H-protein [Hiraga et al., 1981]. Unlike other patients with NKH, this patient showed progressive deterioration and extensive spongy degeneration of white matter with marked gliosis on postmortem examination [Trauner et al., 1981]. It may be that *GCSH* mutations will be found in patients with atypical NKH rather than the more readily recognized clinical form of NKH.

Seven of 32 *GLDC* missense mutations were clustered in exon 19 (Fig. 2). Glycine decarboxylase consists of 1,020 amino acids, and exon 19 encodes 37 of 1,020 amino acids (3.6%), that is, 22% of the *GLDC* missense mutations were clustered in only 3.6% of the protein-coding region. Two octapeptides encoded in exon 19–His749 to Phe756 (HLNLHKTF) and Pro759 to Gly766 (PHGGGGPG)–are perfectly conserved in humans, chickens, peas, and *E. coli*. Crystal structure analysis revealed that His749, Asn751, His753, Lys754, and His760 (underlined) formed an active-site pocket of the GLDC enzyme [Nakai et al., 2005], and the cofactor of GLDC, pyridoxal phosphate, was covalently bound to Lys754 [Fujiwara et al., 1987]. Amino acid changes in this conserved region frequently abolish GLDC enzyme activity, which may be a possible explanation for the high incidence of *GLDC* missense mutations in this region.

Patients P107 and P108 were homozygous for the p.A389V mutation, while patient P104 was a compound heterozygote of the p.A389V mutation and a null mutation, c.1443insG (Table 1). The p.A389V mutation had approximately 8% residual activity in the COS7 expression analysis [Dinopoulos et al., 2005]. Patients P107 and P108 did not present with comas or seizures in the neonatal period, but exhibited developmental delay and abnormal behaviors that developed with age. In contrast, Patient P104 had a typical presentation of the neonatal form of NKH, but subsequently the course of the disease was less severe. The presence of the pA389V mutant allele, which allows some residual enzyme activity, may explain this milder phenotype of classic NKH. The clinical course of P104 resembled those of P6 and P19, who were expected to have 5–8% residual activity by the in vitro expression analysis [Kure et al., 2004]. These results suggest that only a few-percent difference in GCS residual activity dramatically alters the clinical picture, such as age of onset and prognosis. A previous enzymatic study of patients with neonatal and infantile NKH supports this suggestion [Hayasaka et al., 1987]. GCS activities ranged from 0 to 0.7 nmoles of CO_2 formed/mg protein/hr in the neonatal type, while it ranged from 0.7 to 1.4 in the infantile type (for which the control range was 3.9–5.2). However, an exception was observed. Both P69 and P50 were compound heterozygotes of *GLDC* exon 1 deletion and p.G771R. Patient P69 manifested typical symptoms on the second day of life, whereas Patient P50 did not develop symptoms until 3 months of age. Thus far, residual activity is a major determinant of the clinical course, but it is probably modified by environmental factors and/or genotypes of other than the GCS genes.

Elucidation of the responsible gene(s) for late-onset NKH, and screening for deletions in all *GLDC* exons are needed to establish a more complete picture of the genetic background and develop the genotype–phenotype relationships in NKH.

ACKNOWLEDGMENTS

We are grateful to the families who participated in this work. We thank Dr. Avihu Boneh (Royal Children's Hospital, Melbourne), Dr. Helena Haekansson (Lalmar Central Hospital, Sweden), Dr. Shiro Tono-Oka (Kagoshima City Hospital, Japan), Dr. Toshimitsu Takayanagi (National Hospital Organization Saga National Hospital, Japan), Dr. Mitsuru Kubota (Hokkaido University Hospital, Japan), and Dr. Masaki Takayanagi (Chiba Children's Hospital, Japan) for referring the NKH patients.

REFERENCES

Bank WJ, Morrow G 3rd. 1972. A familial spinal cord disorder with hyperglycinemia. Arch Neurol 27:136–144.

Boneh A, Korman SH, Sato K, Kanno J, Matsubara Y, Lerer I, Ben-Neriah Z, Kure S. 2005. A single nucleotide substitution that abolishes the initiator methionine codon of the GLDC gene is prevalent among patients with glycine encephalopathy in Jerusalem. J Hum Genet 50:230–234.

Christodoulou J, Kure S, Hayasaka K, Clarke JT. 1993. Atypical nonketotic hyperglycinemia confirmed by assay of the glycine cleavage system in lymphoblasts. J Pediatr 123:100–102.

Dinopoulos A, Kure S, Chuck G, Sato K, Gilbert DL, Matsubara Y, Degrauw T. 2005. Glycine decarboxylase mutations: a distinctive phenotype of nonketotic hyperglycinemia in adults. Neurology 64:1255–1257.

Ellaway CJ, Mundy H, Lee PJ. 2001. Successful pregnancy outcome in atypical hyperglycinaemia. J Inherit Metab Dis 24: 599–600.

Flannery DB, Pellock J, Bousounis D, Hunt P, Nance C, Wolf B. 1983. Nonketotic hyperglycinemia in two retarded adults: a mild form of infantile nonketotic hyperglycinemia. Neurology 33: 1064–1066.

Flusser H, Korman SH, Sato K, Matsubara Y, Galil A, Kure S. 2005. Mild glycine encephalopathy (NKH) in a large kindred due to a silent exonic GLDC splice mutation. Neurology 64: 1426–1430.

Fujiwara K, Okamura-Ikeda K, Motokawa Y. 1987. Amino acid sequence of the phosphopyridoxyl peptide from P-protein of the chicken liver glycine cleavage system. Biochem Biophys Res Commun 149:621–627.

Fujiwara K, Suzuki M, Okumachi Y, Okamura-Ikeda K, Fujiwara T, Takahashi E, Motokawa Y. 1999. Molecular cloning, structural characterization and chromosomal localization of human lipoyltransferase gene. Eur J Biochem 260:761–767.

Hamosh A, Johnston MV. 2001. Nonketotic hyperglycinemia. In: Scriver CR, Beaudet AL, Sly WS, Valle D, editors. The metabolic and molecular bases of inherited disease, vol 2. New York: McGraw-Hill. p 2065–2078.

Hayasaka K, Tada K, Fueki N, Nakamura Y, Nyhan WL, Schmidt K, Packman S, Seashore MR, Haan E, Danks DM, Schutgems RBH. 1987. Nonketotic hyperglycinemia: analyses of glycine cleavage system in typical and atypical cases. J Pediatr 110:873–877.

Hiraga K, Kochi H, Hayasaka K, Kikuchi G, Nyhan WL. 1981. Defective glycine cleavage system in nonketotic hyperglycinemia. Occurrence of a less active glycine decarboxylase and an abnormal aminomethyl carrier protein. J Clin Invest 68: 525–534.

Hong YS, Kerr DS, Craigen WJ, Tan J, Pan Y, Lusk M, Patel MS. 1996. Identification of two mutations in a compound heterozygous child with dihydrolipoamide dehydrogenase deficiency. Hum Mol Genet 5:1925–1930.

Hoover-Fong JE, Shah S, Van Hove JL, Applegarth D, Toone J, Hamosh A. 2004. Natural history of nonketotic hyperglycinemia in 65 patients. Neurology 63:1847–1853.

Isobe M, Koyata H, Sakakibara T, Momoi-Isobe K, Hiraga K. 1994. Assignment of the true and processed genes for human glycine decarboxylase to 9p23-24 and 4q12. Biochem Biophys Res Commun 203:1483–1487.

Kikuchi G. 1973. The glycine cleavage system: composition, reaction mechanism, and physiological significance. Mol Cell Biochem 1:169–187.

Korman SH, Gutman A. 2002. Pitfalls in the diagnosis of glycine encephalopathy (non-ketotic hyperglycinemia). Dev Med Child Neurol 44:712–720.

Korman SH, Boneh A, Ichinohe A, Kojima K, Sato K, Ergaz Z, Gomori JM, Gutman A, Kure S. 2004. Persistent NKH with transient or absent symptoms and a homozygous GLDC mutation. Ann Neurol 56:139–143.

Kume A, Koyata H, Sakakibara T, Ishiguro Y, Kure S, Hiraga K. 1991. The glycine cleavage system. Molecular cloning of the chicken and human glycine decarboxylase cDNAs and some characteristics involved in the deduced protein structures. J Biol Chem 266:3323–3329.

Kure S, Narisawa K, Tada K. 1991. Structural and expression analyses of normal and mutant mRNA encoding glycine decarboxylase: three-base deletion in mRNA causes nonketotic hyperglycinemia. Biochem Biophys Res Commun 174: 1176–1182.

Kure S, Takayanagi M, Narisawa K, Tada K, Leisti J. 1992. Identification of a common mutation in Finnish patients with nonketotic hyperglycinemia. J Clin Invest 90:160–164.

Kure S, Mandel H, Rolland MO, Sakata Y, Shinka T, Drugan A, Boneh A, Tada K, Matsubara Y, Narisawa K. 1998a. A missense mutation (His42Arg) in the T-protein gene from a large Israeli-Arab kindred with nonketotic hyperglycinemia. Hum Genet 102:430–434.

Kure S, Shinka T, Sakata Y, Osamu N, Takayanagi M, Tada K, Matsubara Y, Narisawa K. 1998b. A one-base deletion (183delC) and a missense mutation (D276H) in the T-protein gene from a Japanese family with nonketotic hyperglycinemia. J Hum Genet 43:135–137.

Kure S, Kojima K, Kudo T, Kanno K, Aoki Y, Suzuki Y, Shinka T, Sakata Y, Narisawa K, Matsubara Y. 2001. Chromosomal localization, structure, single-nucleotide polymorphisms, and expression of the human H-protein gene of the glycine cleavage system (GCSH), a candidate gene for nonketotic hyperglycinemia. J Hum Genet 46:378–384.

Kure S, Kojima K, Ichinohe A, Maeda T, Kalmanchey R, Fekete G, Berg SZ, Filiano J, Aoki Y, Suzuki Y, Izumi T, Matsubara Y. 2002. Heterozygous GLDC and GCSH gene mutations in transient neonatal hyperglycinemia. Ann Neurol 52:643–646.

Kure S, Ichinohe A, Kojima K, Sato K, Kizaki Z, Inoue F, Yamanaka C, Matsubara Y. 2004. Mild variant of nonketotic hyperglycinemia with typical neonatal presentations: mutational and in vitro expression analyses in two patients. J Pediatr 144: 827–829.

Lane RJ, Dick JP, de Belleroche J. 1991. Glycine and neurodegenerative disease. Lancet 337:732–733.

Lane RJ, Virgo L, Lantos PL, de Belleroche J. 1998. A case of multiple system atrophy with hyperglycinaemia due to a selective deficiency of glycine transporter mRNA. Neuropathol Appl Neurobiol 24:353–358.

Leegwater PA, Vermeulen G, Konst AA, Naidu S, Mulders J, Visser A, Kersbergen P, Mobach D, Fonds D, van Berkel CG, Lemmers RJ, Frants RR, Oudejans CB, Schutgens RB, Pronk JC, van der Knaap MS. 2001. Subunits of the translation initiation factor eIF2B are mutant in leukoencephalopathy with vanishing white matter. Nat Genet 29:383–388.

Luder AS, Davidson A, Goodman SI, Greene CL. 1989. Transient nonketotic hyperglycinemia in neonates. J Pediatr 114: 1013–1015.

Mauillon JL, Michel P, Limacher JM, Latouche JB, Dechelotte P, Charbonnier F, Martin C, Moreau V, Metayer J, Paillot B, Frebourg T. 1996. Identification of novel germline hMLH1 mutations including a 22 kb Alu-mediated deletion in patients with familial colorectal cancer. Cancer Res 56:5728–5733.

Nakai T, Nakagawa N, Maoka N, Masui R, Kuramitsu S, Kamiya N. 2005. Structure of P-protein of the glycine cleavage system: implications for nonketotic hyperglycinemia. EMBO J 24: 1523–1536.

Nanao K, Okamura-Ikeda K, Motokawa Y, Danks DM, Baumgartner ER, Takada G, Hayasaka K. 1994a. Identification of the mutations in the T-protein gene causing typical and atypical nonketotic hyperglycinemia. Hum Genet 93:655–658.

Nanao K, Takada G, Takahashi E, Seki N, Komatsu Y, Okamura-Ikeda K, Motokawa Y, Hayasaka K. 1994b. Structure and chromosomal localization of the aminomethyltransferase gene (AMT). Genomics 19:27–30.

Ohya Y, Ochi N, Mizutani N, Hayakawa C, Watanabe K. 1991. Nonketotic hyperglycinemia: treatment with NMDA antagonist and consideration of neuropathogenesis. Pediatr Neurol 7: 65–68.

Okamura-Ikeda K, Ohmura Y, Fujiwara K, Motokawa Y. 1993. Cloning and nucleotide sequence of the gcv operon encoding the *Escherichia coli* glycine-cleavage system. Eur J Biochem 216: 539–548.

Pousi B, Hautala T, Heikkinen J, Pajunen L, Kivirikko KI, Myllyla R. 1994. Alu-Alu recombination results in a duplication of seven exons in the lysyl hydroxylase gene in a patient with the type VI variant of Ehlers-Danlos syndrome. Am J Hum Genet 55:899–906.

Sakata Y, Owada Y, Sato K, Kojima K, Hisanaga K, Shinka T, Suzuki Y, Aoki Y, Satoh J, Kondo H, Matsubara Y, Kure S. 2001. Structure and expression of the glycine cleavage system in rat central nervous system. Brain Res Mol Brain Res 94:119–130.

Schiffmann R, Kaye EM, Willis JK 3rd, Africk D, Ampola M. 1989. Transient neonatal hyperglycinemia. Ann Neurol 25: 201–203.

Sellner L, Edkins E, Greed L, Lewis B. 2005. Detection of mutations in the glycine decarboxylase gene in patients with nonketotic hyperglycinaemia. Mol Genet Metab 84:167–171.

Singer HS, Valle D, Hayasaka K, Tada K. 1989. Nonketotic hyperglycinemia: studies in an atypical variant. Neurology 39: 286–288.

Steiman GS, Yudkoff M, Berman PH, Blazer-Yost B, Segal S. 1979. Late-onset nonketotic hyperglycinemia and spinocerebellar degeneration. J Pediatr 94:907–911.

Stoppa-Lyonnet D, Duponchel C, Meo T, Laurent J, Carter PE, Arala-Chaves M, Cohen JH, Dewald G, Goetz J, Hauptmann G, Lagrue G, Lesavre P, Lopez-Trascasa M, Misiano G, Moraine C, Sobel A, Spōth PJ, Tosi M. 1991. Recombinational biases in the rearranged C1-inhibitor genes of hereditary angioedema patients. Am J Hum Genet 49:1055–1062.

Suzuki Y, Ueda H, Toribe Y. 2001. [Proton MR spectroscopy of nonketotic hyperglycinemia]. No To Hattatsu 33:422–425.

Tada K, Narisawa K, Yoshida T, Yokoyama K, Nakagawa H, Tanno K, Mochizuki K, Arakawa T, Yoshida T, Kikuchi G. 1969. Hyperglycinemia: a defect in glycine cleavage reaction. Tohoku J Exp Med 98:289–296.

Tada K, Hayasaka K. 1987. Non-ketotic hyperglycinaemia: clinical and biochemical aspects. Eur J Pediatr 146:221–227.

Takayanagi M, Kure S, Sakata Y, Kurihara Y, Ohya Y, Kajita M, Tada K, Matsubara Y, Narisawa K. 2000. Human glycine decarboxylase gene (GLDC) and its highly conserved processed pseudogene (psiGLDC): their structure and expression, and the identification of a large deletion in a family with nonketotic hyperglycinemia. Hum Genet 106:298–305.

Toone JR, Applegarth DA, Coulter-Mackie MB, James ER. 2000. Biochemical and molecular investigations of patients with nonketotic hyperglycinemia. Mol Genet Metab 70:116–121.

Toone JR, Applegarth DA, Coulter-Mackie MB, James ER. 2001. Recurrent mutations in P- and T-proteins of the glycine cleavage complex and a novel T-protein mutation (N145I): a strategy for the molecular investigation of patients with nonketotic hyperglycinemia (NKH). Mol Genet Metab 72:322–325.

Toone JR, Applegarth DA, Kure S, Coulter-Mackie MB, Sazegar P, Kojima K, Ichinohe A. 2002. Novel mutations in the P-protein (glycine decarboxylase) gene in patients with glycine encephalopathy (non-ketotic hyperglycinemia). Mol Genet Metab 76: 243–249.

Toone JR, Applegarth DA, Levy HL, Coulter-Mackie MB, Lee G. 2003. Molecular genetic and potential biochemical characteristics of patients with T-protein deficiency as a cause of glycine encephalopathy (NKH). Mol Genet Metab 79: 272–280.

Trauner DA, Page T, Greco C, Sweetman L, Kulovich S, Nyhan WL. 1981. Progressive neurodegenerative disorder in a patient with nonketotic hyperglycinemia. J Pediatr 98:272–275.

Turner SR, Ireland R, Rawsthorne S. 1992. Cloning and characterization of the P subunit of glycine decarboxylase from pea (*Pisum sativum*). J Biol Chem 267:5355–5360.

van der Knaap MS, Wevers RA, Kure S, Gabreels FJ, Verhoeven NM, van Raaij-Selten B, Jaeken J. 1999. Increased cerebrospinal fluid glycine: a biochemical marker for a leukoencephalopathy with vanishing white matter. J Child Neurol 14:728–731.

von Wendt L, Hirvasniemi A, Simila S. 1979. Nonketotic hyperglycinemia. A genetic study of 13 Finnish families. Clin Genet 15:411–417.

Wiltshire EJ, Poplawski NK, Harrison JR, Fletcher JM. 2000. Treatment of late-onset nonketotic hyperglycinaemia: effectiveness of imipramine and benzoate. J Inherit Metab Dis 23:15–21.

Zafra F, Aragon C, Gimenez C. 1997. Molecular biology of glycinergic neurotransmission. Mol Neurobiol 14:117–142.

BRAIN RESEARCH 1071 (2006) 24-33

available at www.sciencedirect.com

SCIENCE DIRECT®

www.elsevier.com/locate/brainres

BRAIN RESEARCH

Research Report

De novo and salvage pathways of DNA synthesis in primary cultured neurall stem cells

Kenichi Sato[a,b], *Junko Kanno*[a], *Teiji Tominaga*[b], *Yoichi Matsubara*[a,c], *Shigeo Kure*[a,c,*]

[a]*Department of Medical Genetics, Tohoku University School of Medicine, 1-1 Seiryo-machi, Aobaku, Sendai 980-8574, Japan*
[b]*Department of Neurosurgery, Tohoku University School of Medicine, Sendai, Japan*
[c]*Tohoku University 21st Century COE Program "Comprehensive Research and Education Center for Planning of Drug Development and Clinical Evaluation," Sendai, Japan*

ARTICLE INFO

Article history:
Accepted 6 November 2005
Available online 10 January 2006

Keywords:
Neural stem cell
Neurosphere
Proliferation
DNA synthesis pathway
Folic acid

ABSTRACT

We studied the de novo and salvage pathways of DNA synthesis in sphere-forming neural stem cells obtained from mouse embryos by a neurosphere method. The former pathway needs folic acid (FA) for nucleotide biosynthesis, while the latter requires deoxyribonucleosides (dNS). We examined the proliferative activity of sphere-forming cells in E14.5 embryos by counting the number of spheres formed in media that lacked FA and/or dNS. Proliferation failure and apoptosis occurred in a deficient medium lacking of both FA and dNS. Spheres formed in the deficient medium supplemented with dNS, without FA, did not produce neuron, but rather only seem to generate astrocytes and oligodendrocytes when plated under differentiation condition in culture. On the other hand, a subpopulation of cultured cells formed spheres in the deficient medium supplemented with FA alone in an appropriate concentration, and did possess the self-renewing and multipotential characteristics of neural stem cells. Spheres formed in the media containing low dose Azathioprine and methotrexate, inhibitors of de novo DNA synthesis, were selectively prevented from producing neurons even in the presence of FA. These results suggested that activating de novo DNA synthesis was needed for neural stem cells to proliferate with multipotentiality.

* *Corresponding author*. Department of Medical Genetics, Tohoku University School of Medicine, 1-1 Seiryo-machi, Aobaku, Sendai 980-8574, Japan. Fax: +81 22 717 8142.
E-mail address: skure@mail.tains.tohoku.ac.jp (S. Kure).

0006-8993/$ – see front matter © 2005 Elsevier B.V. All rights reserved.
doi:10.1016/j.brainres.2005.11.039

Abbreviations:
FA, folic acid
dNS, deoxyribonucleosides
dNTPs, deoxynucleoside triphosphates
dAdo, 2′-deoxyadenosine
dCyd, 2′-deoxycytidine
dGuo, 2′-deoxyguanosine
Thy, thymidine
AZP, azathioprine
MTX, methotrexate
NTD, neural tube defect
DIV, days in vitro
GFAP, glial fibrillary acidic protein

1. Introduction

Normal CNS development involves the sequential differentiation of multipotent stem cells. Alteration in the number of stem cells or their proliferative capability has major effects on the appropriate development of the nervous system (Sommer and Rao, 2002). One of the essential steps for the proliferation of stem cells is DNA synthesis. DNA precursors, i.e., nucleotides, are synthesized through two metabolic pathways referred to as de novo pathway and salvage pathway (Fig. 1). In the de novo pathway, deoxynucleoside triphosphates (dNTPs) are generated in multiple steps from 5-phosphoribosyl-1-pyrophosphate, glutamine, glycine, aspartate, and folic acid (FA). Since animal cells cannot synthesize FA, FA supplementation into their culture media is required for activating de novo DNA synthesis (Murray et al., 1999). In the salvage pathway, dNTPs are produced in single steps from exogenous and endogenous deoxyribonucleosides (dNS). The de novo pathway is predominant in normal differentiated tissues, whereas the salvage pathway is activated in rapidly proliferating tissues, including fetal and regenerative tissues and cancer cells (Hatse et al., 1999). Previous studies functionally evaluated the DNA synthesis in erythroblasts using culture media deficient of FA and/or dNS, and that indicated that erythroblasts underwent apoptosis during S phase in the lack of both FA and dNS (James et al., 1994; Koury and Horne, 1994; Koury et al., 2000). To date, the DNA synthesis pathway employed in neural stem cells remains uninvestigated.

Reynolds and Weiss (1996) reported that neural stem cells could be established from rodent brains by the neurosphere culture method. Using the neurosphere method, single

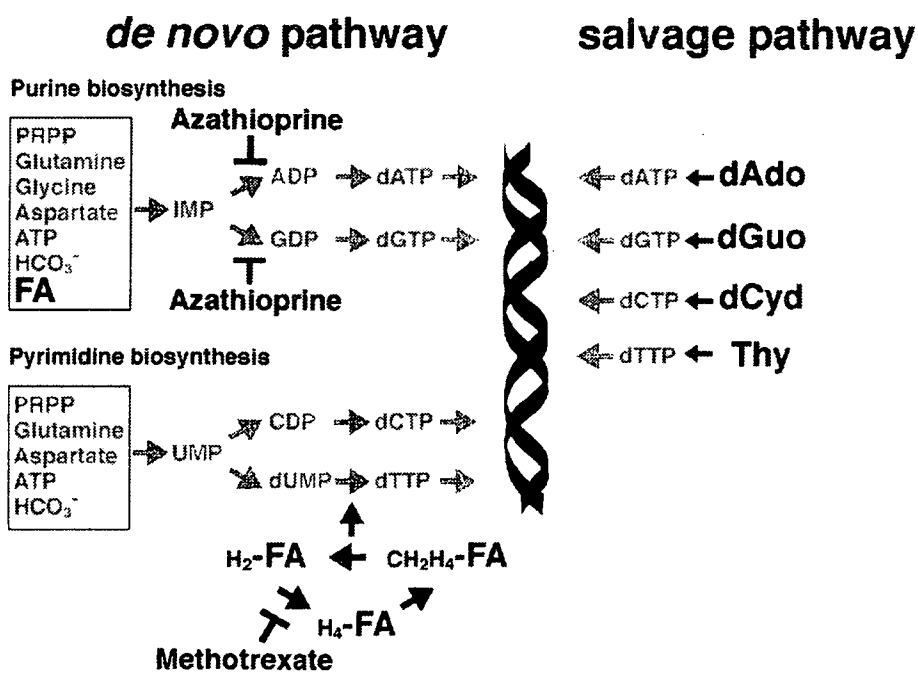

Fig. 1 – De novo and salvage biosynthesis of DNA. DNA is synthesized through two pathways: the de novo pathway (left panel) and salvage pathway (right panel). Abbreviations: IMP, inosinic acid; UMP, uridine monophosphate; dAdo, 2′-deoxyadenosine; dCyd, 2′-deoxycytidine; dGuo, 2′-deoxyguanosine; Thy, thymidine; H_2-FA, dihydrofolate; H_4-FA, tetrahydrofolate; CH_2H_4-FA, N^5,N^{10}-methylenetetrahydrofolate.

neural stem cells can be selectively expanded in a chemically defined medium containing epidermal growth factor (EGF), fibroblast growth factor 2 (FGF-2), or both, giving rise to floating spheroid cell aggregates called neurospheres. Since D-MEM/F-12, the commonly used medium for the neurosphere culture, contains both FA and two kinds of dNS, namely, thymidine (Thy) and hypoxanthine, the pathway of DNA synthesis that operates in the proliferation of neural stem cells remains unknown.

In this report, we performed the neurosphere method by using a custom-prepared D-MEM/F-12 medium that lacked FA and/or dNS for the functional evaluation of DNA synthesis pathways in embryonic sphere-forming neural stem cells. We examined the efficiency of the sphere formation and characterized the multipotency of the neural stem cells by in vitro differentiation analysis. Specific inhibitors of de novo DNA synthesis were used for the further characterization of sphere-forming cells. These approaches enabled us, for the first time, to perform the functional evaluation of DNA synthesis in neural stem cells.

2. Results

2.1. *Sphere formation derived from the E14.5 mouse striata in FA+/dNS− or FA−/dNS+ media*

To determine the DNA synthesis pathway utilized by embryonic neural stem cells for proliferation, we cultured neurospheres derived from the E14.5 mouse striata in D-MEM/F-12 medium lacking the precursors of DNA synthesis, defined as a deficient medium. We supplemented the deficient medium with varying amounts of FA, as a precursor for the de novo pathway, or dNS (equimolar addition of dAdo, dGuo, dCyd, and Thy), as precursors for the salvage pathway. In the deficient medium, designated as FA−/dNS− medium, no sphere was formed, and the condensation of cultured cells and the fragmentation of nuclei, which are characteristic of apoptosis, were observed. Terminal deoxynucleotidyl transferase-mediated dUTP-biotin nick end labeling (TUNEL) showed increased TUNEL-positive cells (mean ± SEM, 56.7% ± 1.5%; $n = 4$) in the deficient medium when compared with those in the deficient medium containing 10 μM FA and 50 μM dNS (29.2% ± 1.1%, $n = 5$, $P < 0.01$) (data not shown). These results suggested that cultured cells did not proliferate and underwent apoptosis in the medium without the precursors of DNA synthesis. In the medium containing only FA, maximum number of spheres was formed with 10 μM FA (Fig. 2A). In the absence of FA, peak sphere formation efficiency with each dNS was observed at a concentration of 50 μM (Fig. 2B). We defined the culture condition of 10 μM FA without dNS as FA+/dNS−. Similarly, the condition in which the culture was supplemented with 50 μM of each dNS without FA was designated as FA−/dNS+.

2.2. *Sphere-forming activity in the presence of various combinations of dNS*

Eukaryotes generally have converting enzymes among purine and pyrimidine deoxyribonucleosides (Murray et al., 1999). To determine the precursors of the salvage pathway that are required for sphere formation, we tested 16 different combinations of 10 μM dNS. As shown in Fig. 2C, the combination of dAdo with Thy yielded maximum sphere-forming efficiency and additional supplementation with other dNSs had little effect on the efficiency.

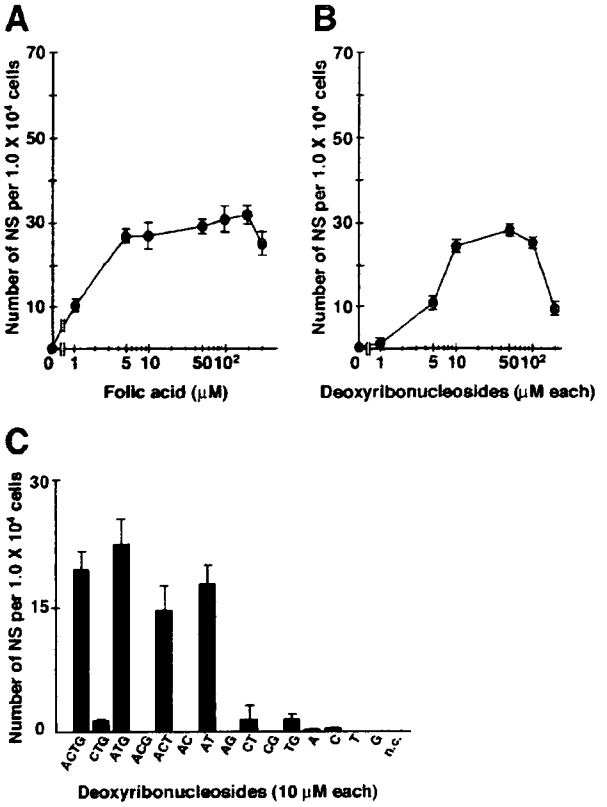

Fig. 2 – (A and B) Dose–response curves of sphere formation cultured for 7 DIV in the deficient medium supplemented with FA (A) or dNS (B). During this developmental period, spheres can be formed in the presence of FA or dNS in an appropriate concentration. (C) The number of spheres cultured for 7 DIV in the deficient medium supplemented with 16 different combinations of deoxyribonucleosides, each at a concentration of 10 μM. Graphs show mean ± SEM number of spheres per 1 × 10^4 cells prepared from the E14.5 mouse striata. Abbreviations: A, 2′-deoxyadenosine; C, 2′-deoxycytidine; G, 2′-deoxyguanosine; T, thymidine.

2.3. *Developmental-stage specific changes of sphere-forming activities under the FA+/dNS− and FA−/dNS+ conditions*

To examine the developmental changes of sphere-forming activities under the FA+/dNS− and FA−/dNS+ conditions, we performed the neurosphere cultures derived from the E12.5 and E16.5 mice striata in the deficient medium supplemented with varying amounts of FA or dNS (Fig. 3). In the cultures derived from the E16.5 striata, nearly the same number of spheres was formed with appropriate concentrations of FA and dNS. However, in the culture derived from

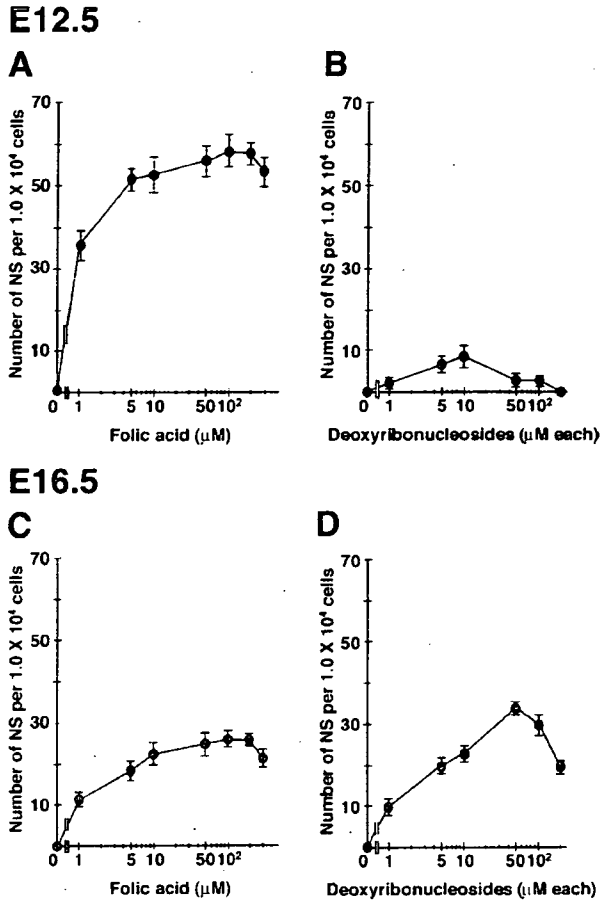

Fig. 3 – Developmental change of dose-response curve of sphere formation, cultured for 7 DIV in the deficient medium supplemented with FA (A and C) or dNS (B and D). Graphs show mean ± SEM number of spheres per 1 × 10^4 cells prepared from E12.5 (A and B) and E16.5 (C and D) mice striata.

E12.5, only a few spheres were formed under the FA−/dNS+ condition.

2.4. *Morphological and immunochemical characterizations of the formed spheres in the FA+/dNS− or FA−/dNS+ media*

Spheres formed under the FA−/dNS+ condition morphologically differed from those formed under the FA+/dNS− condition (Figs. 4A, B). After 7 DIV, the FA+/dNS− spheres were large, smooth, and spherical in shape, while the FA−/dNS+ spheres were small and irregular in shape. The FA+/dNS− spheres were 77.0 ± 3.8 μm (n = 66) in diameter, larger than the FA−/dNS+ spheres (49.8 ± 2.5 μm, n = 78, $P < 0.01$). It is unlikely that both spheres were derived from ciliated cells by their morphological characteristics (Chiasson et al., 1999; Laywell et al., 2000). Immunochemical characterization showed that both spheres were immunopositive for Nestin (a neural progenitor marker), GFAP (an astrocyte marker), and O4 (an oligodendrocyte marker) (Figs. 4C, D, G–J). However, tubulin β III (a neuron marker) positive cells were observed only in the FA+/dNS− spheres (Fig. 4E), and not in the FA−/dNS+ spheres (Fig. 4F), suggesting that cells in the FA−/dNS+ spheres barely differentiated into neurons.

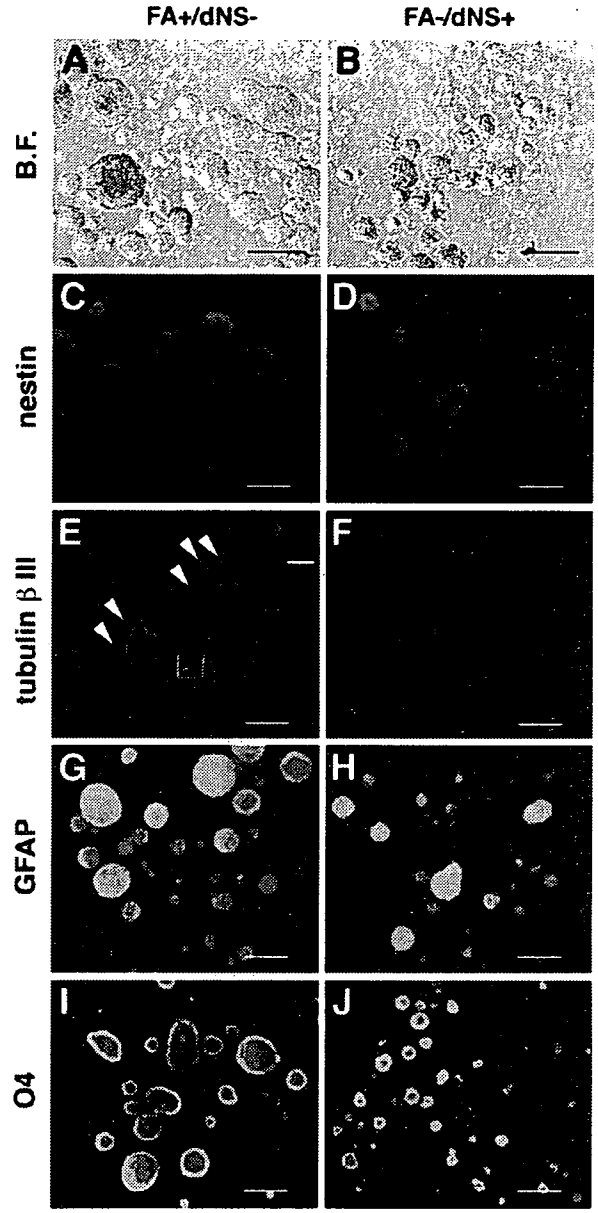

Fig. 4 – FA−/dNS+ spheres contain astrocytes and oligodendrocytes, but not neurons. (A and B) Phase-contrast images of live floating spheres under the FA+/dNS condition (A) and FA−/dNS+ condition (B). (C–J) Immunofluorescence of chemical markers for neural progenitors (nestin, red; C and D), neurons (tubulin β III, red; E and F), astrocytes (GFAP, green; G and H), oligodendrocytes (O4, green; I and J), and nucleus (DAPI, *blue; C–J*) derived from the FA+/dNS− spheres (C, E, G, and I) and FA−/dNS+ spheres (D, F, H, and J). White arrowheads indicate tubulin β III-positive neurons. Inset in panel E is high magnification of a white box. Scale bars: A–J, 200 μm; Inset, 20 μm. Abbreviations: B.F., bright field; GFAP, glial fibrillary acidic protein.

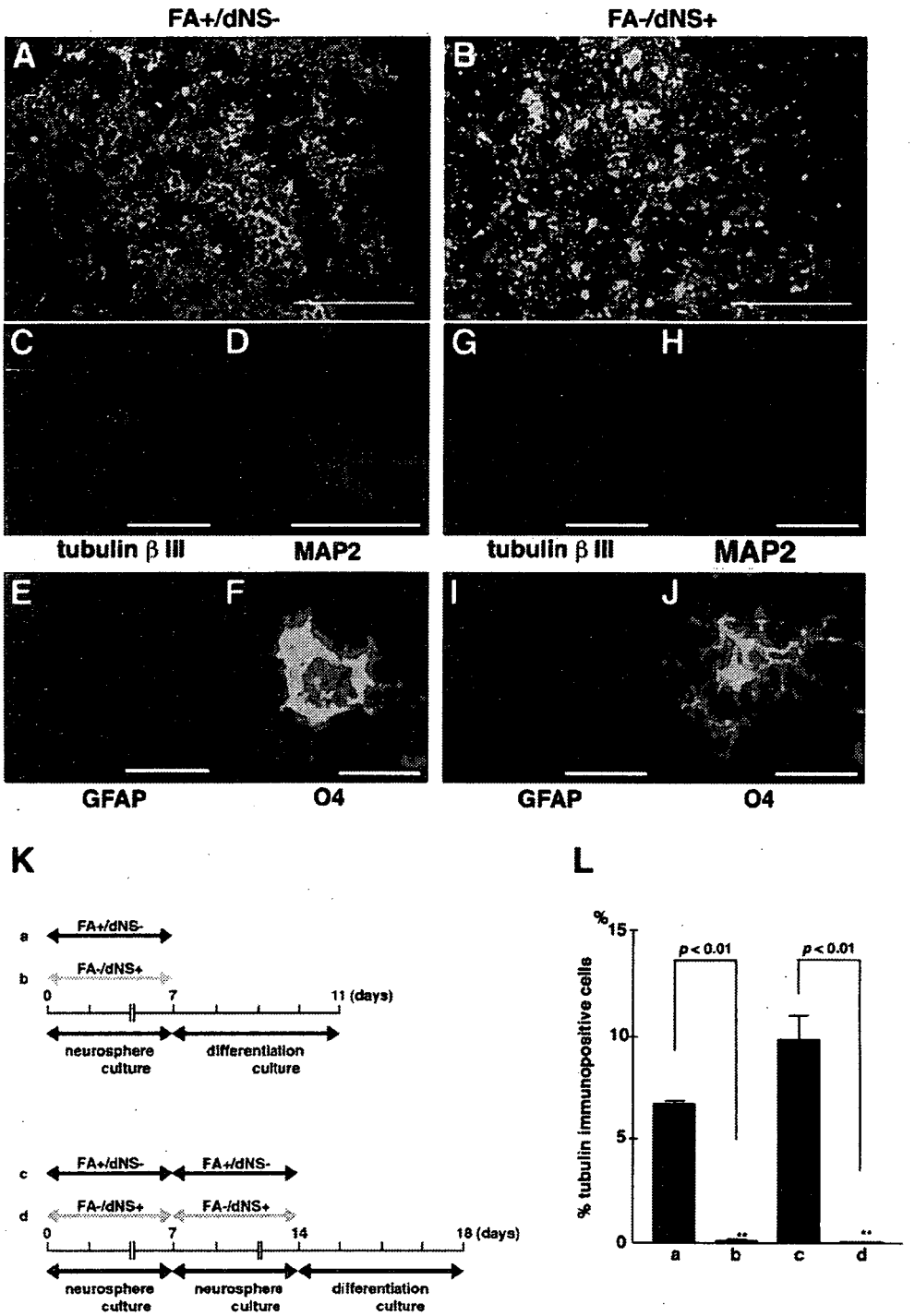

Fig. 5 – Tri-colored immunofluorescence of markers for neurons (tubulin β III, red), astrocytes (GFAP, blue), and oligodendrocytes (O4, *green*) shows that the FA+/dNS– clonal spheres gave rise to different cells expressing markers of all three neural cell types, as depicted in a triple-labeled survey (A), and the details of individual cells of each type (C–F). The FA–/dNS+ spheres gave rise to astrocytes and oligodendrocytes, but not neurons, as shown in a triple-labeled survey (B), which also depicted the details of individual cells (G–J). Scale bars: A, B, 200 μm; C–J, 20 μm. (K) Experimental protocol. The 7-DIV primary culture in the FA–/dNS+ (a) and FA+/dNS– (b) condition was placed under the differentiation condition for 4 DIV (total 11 DIV). (c), The 7-DIV primary culture in the FA+/dNS– medium was placed under the FA+/dNS– condition for 7 DIV (total 14 DIV) and, then, the cultured cells were placed under the differentiation condition for 4 DIV (total 18 DIV). (d) Likewise, the FA–/dNS+ primary culture was placed under the FA–/dNS+ condition and, then, under the differentiation condition. (L) Graph showing mean ± SEM percentage of tubulin β III-immunopositive neurons of the total number of cells per field derived from each protocol. **Significant difference between the two groups ($P < 0.01$).